9-1976

# Calculated Temperature of Grid Lateral Wires in Microwave Power Triodes

Jewell Tucker
*Western Kentucky University*

Tucker,

Jewell G.

1976

# CALCULATED TEMPERATURE OF GRID LATERAL WIRES IN MICROWAVE POWER TRIODES

A THESIS

Presented to

the Faculty of the Department of Physics and Astronomy

Western Kentucky University

Bowling Green, Kentucky

In Partial Fulfillment

of the Requirements for the Degree

Master of Engineering Physics

by

Jewell G. Tucker

September 1976

CALCULATED TEMPERATURE OF GRID LATERAL

WIRES IN MICROWAVE POWER TRIODES

Recommended April 23, 1977
(Date)

George E. Moore
Director of Thesis

Curtis A. Logsdon

N. T. Sips

Approved April 25, 1977
(Date)

Elmer Gray
Dean of the Graduate College

ACKNOWLEDGMENT

The author is indebted to Dr. G.C. Moore, C.A. Logsdon, and Dr. N.F. Six, Western Kentucky University, for their suggestions and assistance in planning this development. Recognition is given to the following Microwave and Imaging Devices Products Section, Tube Products Department, personnel. Conversations with C. Hopper, J.D. Campbell, L.E. Roberts, and C.V. Claypool were very helpful. The proofreading by E.B. Foster and W.U. Shipley, and the computer programming assistance of R.W. Grinker is appreciated. A special thanks to Dorothy Ayres for typing. Finally, this work would not have been possible without the equipment and facilities furnished by the General Electric Company, Tube Products Department, Owensboro, Kentucky.

TABLE OF CONTENTS

Appendix

## LIST OF TABLES

PHOTOGRAPHS

LIST OF FIGURES

# CALCULATED TEMPERATURE OF GRID LATERAL WIRES IN MICROWAVE POWER TRIODES

Jewell G. Tucker September 1976 63 pages

Directed by: G.C. Moore and C.A. Logsdon

Department of Physics and Astronomy Western Kentucky University

In microwave power triodes the grid drive power causes grid lateral wire heating. This development calculates the temperature of the wire as a function of the drive power, physical dimensions and characteristics of the wire material, for the following boundary conditions:

I. Constant grid drive, grid lateral wire of infinite length not connected to a heat sink.

II. Same as I except the wire is of finite length brazed to a grid frame.

III. The grid excitation in the form of pulses, and the grid lateral wire of finite length brazed to a grid frame.

The equations were verified experimentally by calculating the temperature of a rod whose surface was heated in a vacuum and the temperature measured. The equations were also used to estimate the grid drive power necessary to melt tungsten lateral wire in a microwave power triode, GE18651. The repeated use of LaPlace and Fourier transforms, the Dirac impulse function and convolution integral are the principal mathematical tools used to solve the conduction equations.

# INTRODUCTION

In the early days of radio, thermocouples could be welded to the inner-elements of receiving tubes to measure the temperatures. Figure 1 illustrates how the temperature of the grid lateral wire could be determined in a radio receiver power triode.

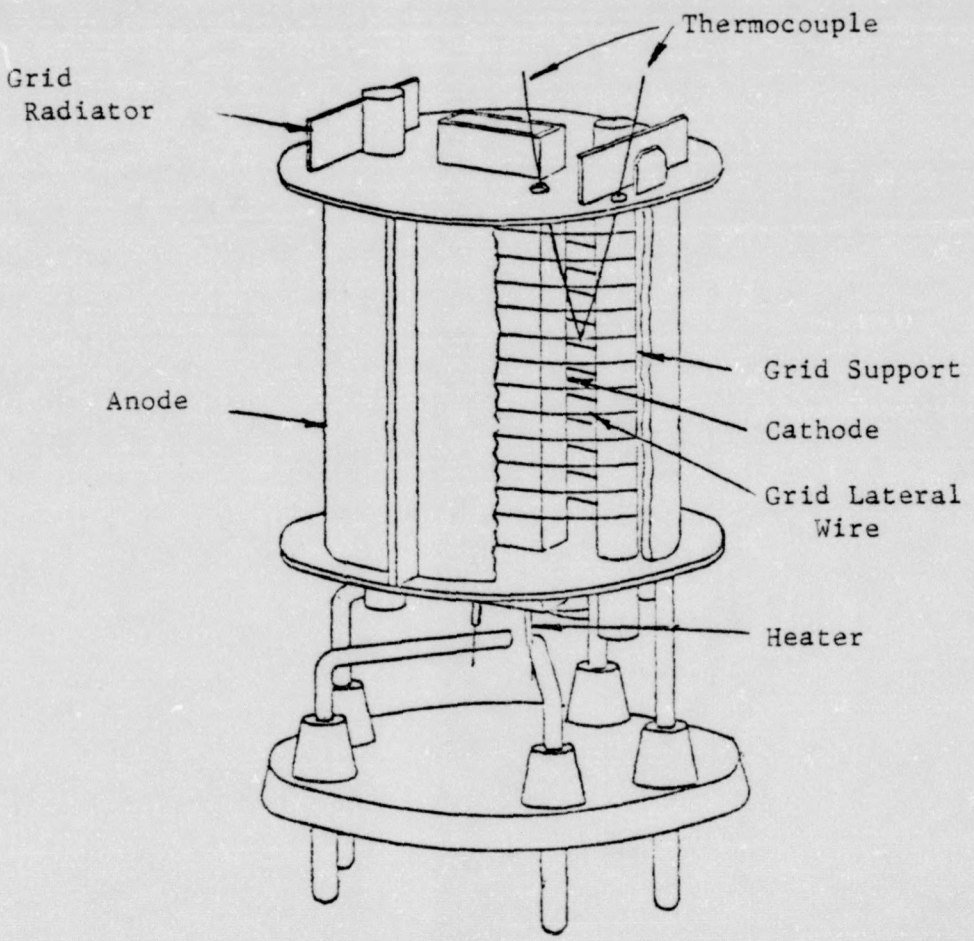


Figure 1 - Radio Receiving Tube With Thermocouple Welded to Grid Lateral Wire

Receiving tubes were improved and this caused the elements and the spacings to be smaller. At television frequencies the thermocouple technique is limited to determining the support rod temperature and estimating the lateral grid wire temperature.

At microwave frequencies, the spacings and elements are so small that thermocouples can only be used to measure the anode and grid ring temperatures external to the tube. These temperatures are not approximations to the grid lateral wire temperatures because of the small diameter of the wire and the thermal impedance between the source and the grid ring.

Table I represents typical power triodes used at radio, television, and microwave frequencies and the element spacing and grid wire diameters.

Table I

Power Triodes Used at Radio, Television, and Microwave Frequencies

| | Tube Type | Spacing of Grid Cathode | Spacing of Grid-Anode | Lateral Grid Wire Diameter |
|---|---|---|---|---|
| Radio | 37 | .025" | .080" | .005" |
| Television | 6J6 | .0045" | .017" | .003" |
| Microwave | GE18651 | .002" | .0132" | .0006" |

The dynamic behavior of a receiving tube, as a function of the grid lateral wire temperature, depends on the application; however, several potential problem areas are:

(1) The grid wires emit electrons at high temperatures, causing instability.

(2) The grid wires evolve contaminants at high temperature that poison the emissive coating on the cathode and reduce the cathode current, output voltage, and power.

(3) The probability of inner-element arcing increases at elevated grid lateral wire temperature.

It has been the purpose of this study to develop equations and a computer program that will calculate the time dependent grid lateral wire temperature in Microwave Planar Power Triodes as a function of the known parameters.

# CHAPTER I

## PHYSICAL MODEL

Microwave Gridded Planar Triodes[1] are used in Phased Array Radar, Airborne Communication Equipment, and numerous other applications requiring high performance and reliability. These systems have placed more stringent requirements on these active devices that convert power at dc up to 10,000,000,000 (10 gigahertz) cycles per second.

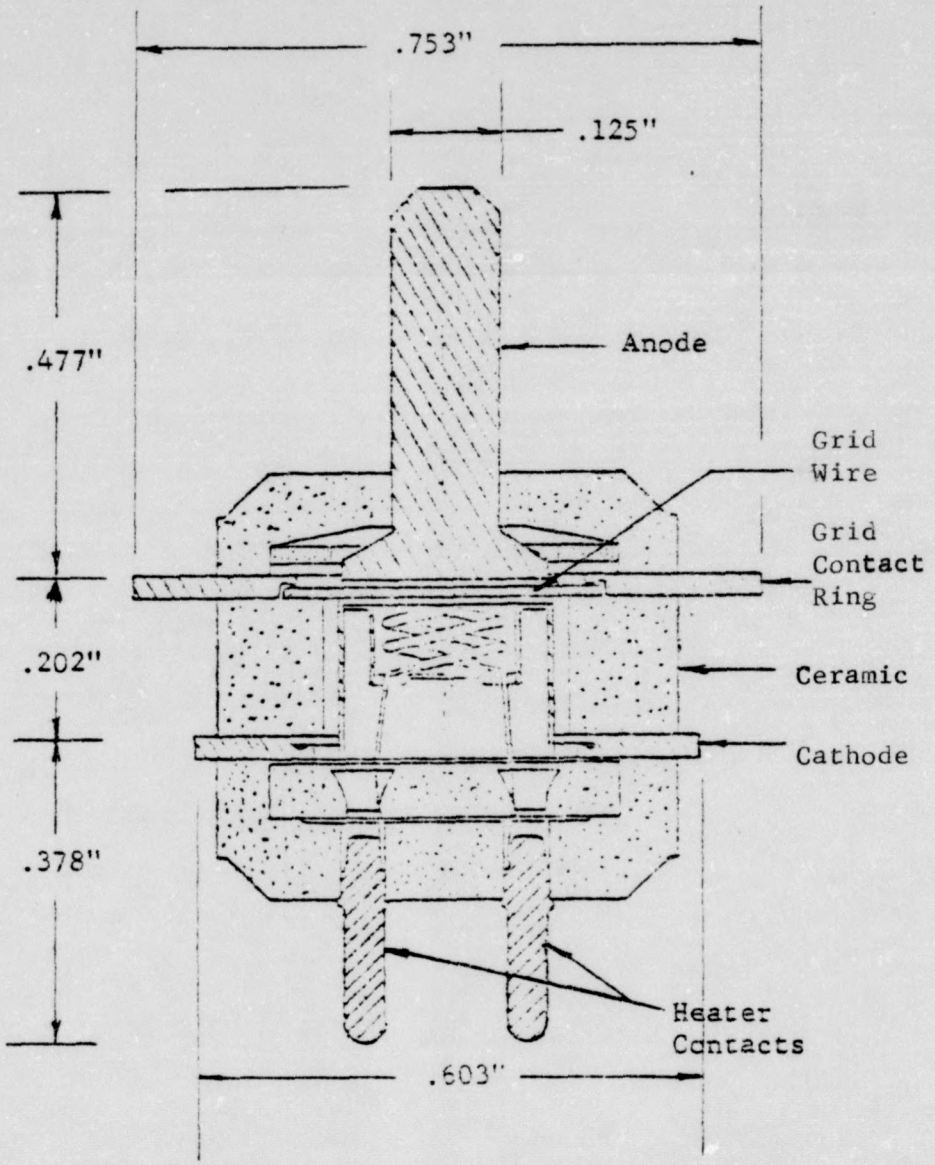


Figure 2 - Planar Ceramic Triode GE18651 Cross Section

Figure 2 is a cross sectional view of the GE18651, a high performance ceramic planar triode, used in airborne communication equipment.

Figure 3 shows the microwave planar triode performance as a function of frequency and cathode current density. To generate these high cathode current densities, it is necessary to excite the grid with a voltage positive relative to the cathode.

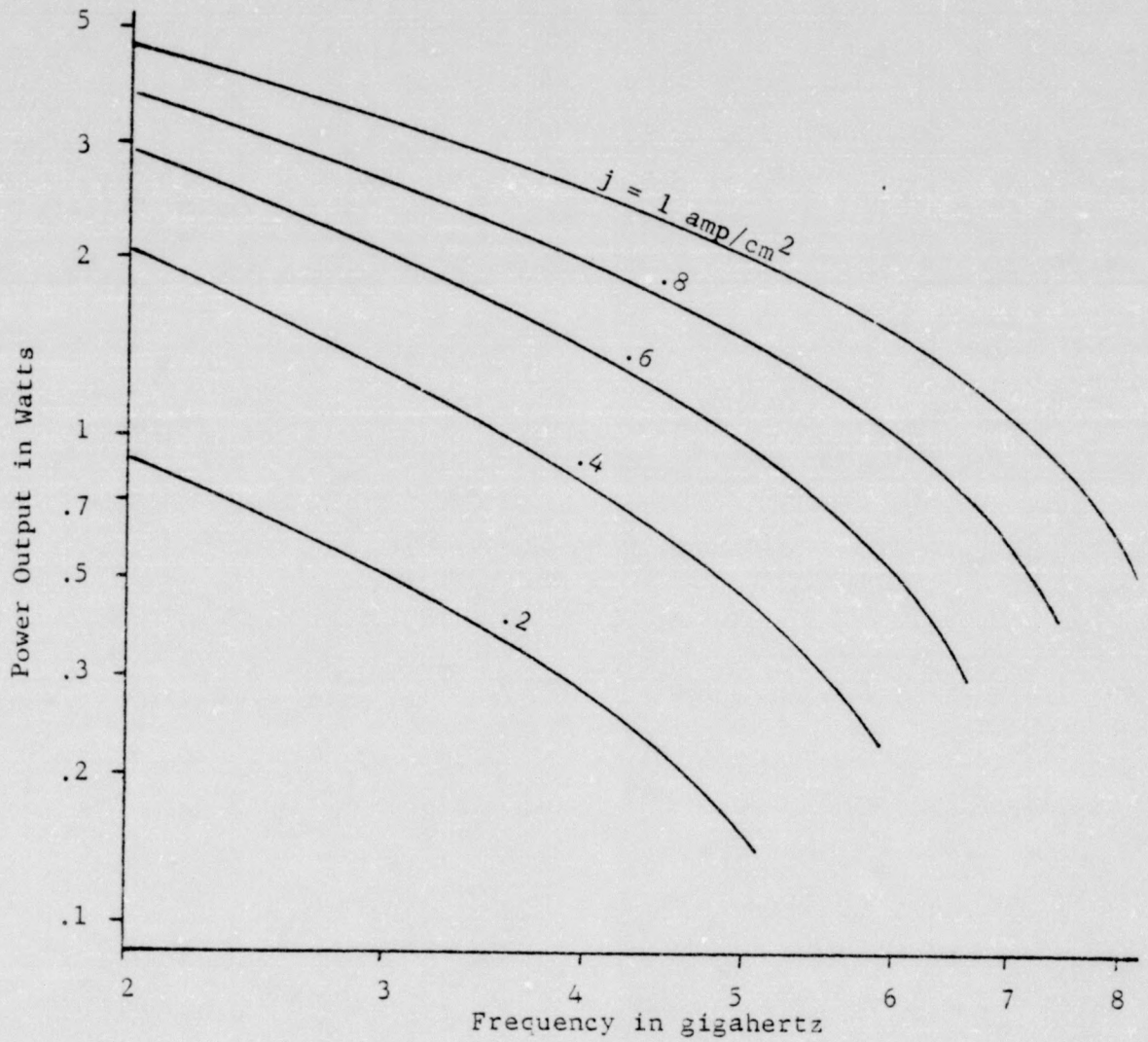


Figure 3 - Microwave Planar Triode Performance at High Current Densities

A magnified sketch of the GE18651 cross section is shown in Figure 4 with a representation of the electron distributions to the anode and grid wires.

The power absorbed by the grid can be calculated by plotting the instantaneous grid voltage and current[2], taken from the constant current curves and multiplied by the transit angle. These are summed for one cycle of excitation. This relation is a nonlinear expression, but if small increments are taken, the calculated grid power is within 10% of the measured value.

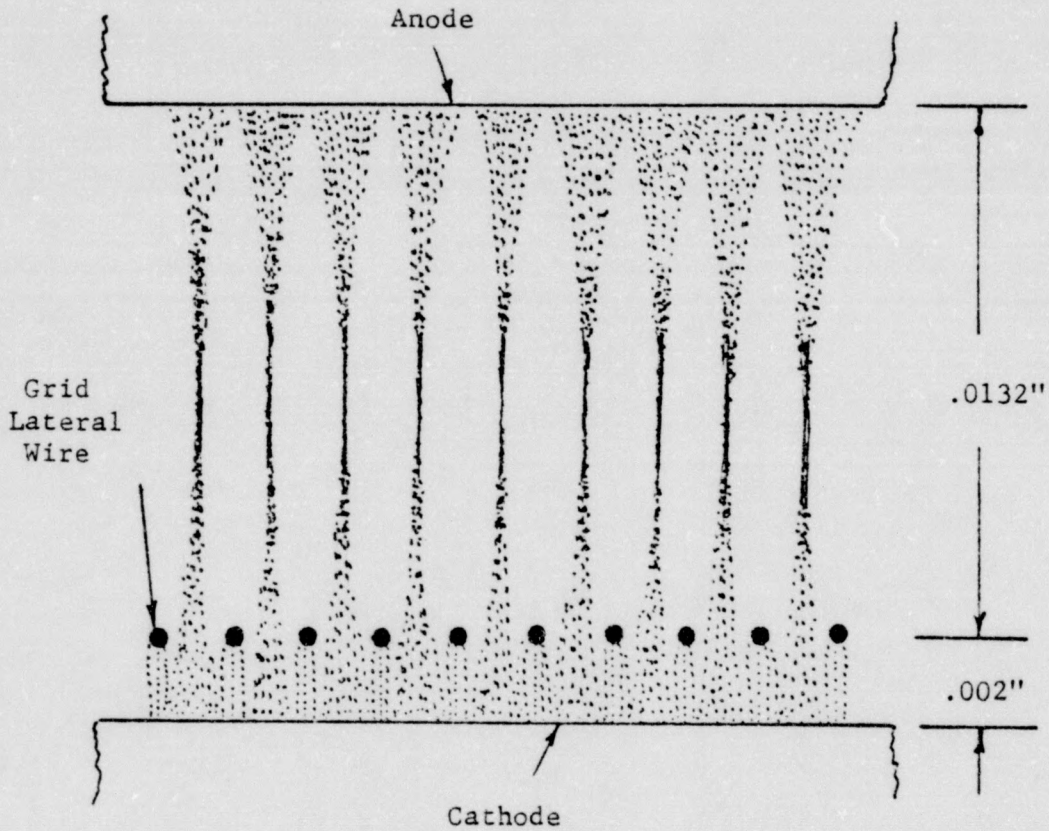


Figure 4 - GE18651 Power Triode Showing Electron Densities to Grid and Anode

Figure 5 shows a sketch of a planar tube grid, tube type GE18651. The grid voltage excitation is applied for three cycles lasting $\tau$ seconds and the pulses repeat at a rate of T seconds.

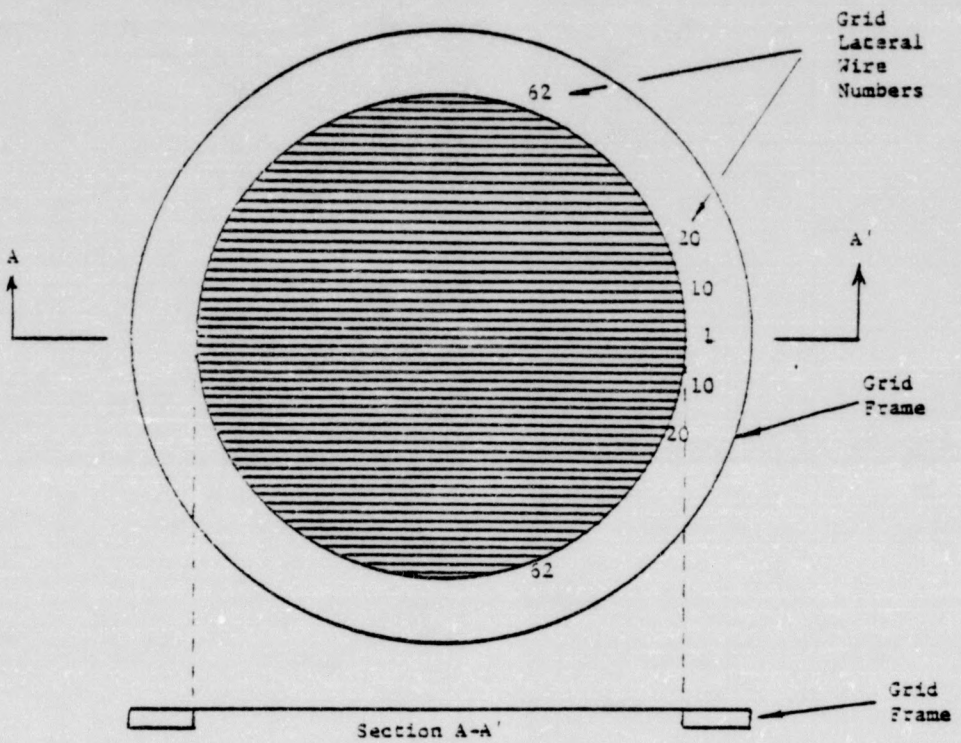


Figure 5(a) - Sketch of Planar Tube Grid

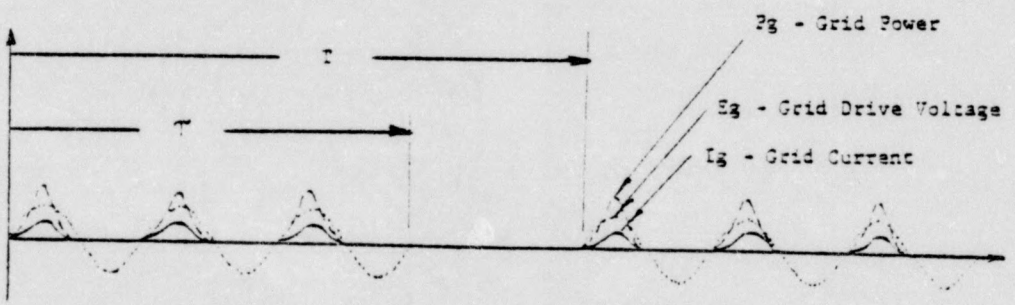


Figure 5(b) - Power Excitation to a Single Grid Lateral Wire Number 1

The grid power can also be measured in a microwave circuit by using a flow-through wattmeter and multiplying by the ratio of grid to anode current. This ratio is to account for the percent of input power that is absorbed by the load in the anode circuit.

In this study, the power absorbed by the grid is assumed to be uniform; that is, the current flow per unit area is the same for Lateral Number 1 as for Lateral Number 62.

The cathode and anode of the GE18651 operate at approximately 860°C and 400°C, respectively, and these elements radiate energy that is absorbed by the grid. The ends of the lateral wire are connected to a frame that acts as a heat sink. In the GE18651 design the grid frame is a tungsten washer that is .040" x .010" in cross section.

The grid excitation and the radiant energy from the cathode and anode suggest a physical model for a grid lateral wire as shown in Figure 6.

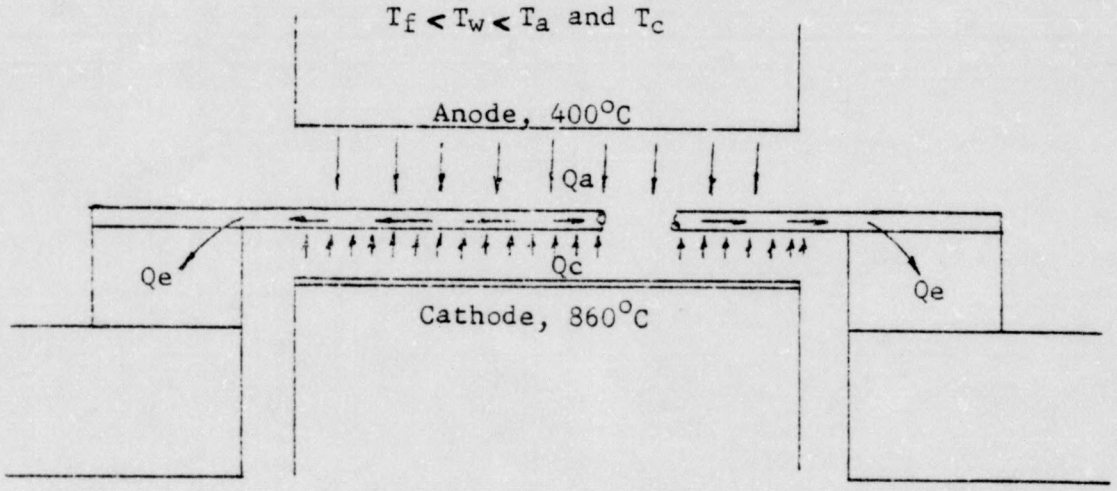


Figure 6 - Heat Flow in a Single Lateral Connected to a Heat Sink

Where

Qa = radiant energy from the anode absorbed by the grid

Qe = heat generated in the grid because of the excitation power

Qc = radiant energy from the cathode absorbed by the grid

Tf = temperature of the grid frame

Tw = temperature of the grid wire

Ta = temperature of the anode

Tc = temperature of the cathode

# CHAPTER II

## MODIFIED PHYSICAL MODEL

The classical field of heat transfer includes conduction, convection, and radiation. In planar receiving tubes, the convection mode is negligible because these devices are high vacuum; that is, less than $10^{-7}$ Torr.

The grid lateral wires are positioned accurately between the cathode and anode surfaces, which are typically 860°C and 400°C, respectively. These elements radiate energy to the lateral wire and cause the wires to attain an estimated steady state temperature of approximately 350°C. This analysis treats the temperature variations of the lateral wire because of the grid drive power and assumes this time dependent temperature change is not a function of the steady state temperature due to the radiation.

The conduction of heat is given by Fourier's[3] generalized conduction equation:

$$\frac{\partial T}{\partial t} = \alpha \nabla^2 T + \frac{\Gamma}{\rho C_p} \qquad (1)$$

where $T$ = temperature

$t$ = time

$\alpha$ = thermal diffusivity

$\nabla$ = operator, gradient

$\Gamma$ = heat generated

$\rho$ = mass density

$C_p$ = specific heat

The internal heat generated, $\Gamma$ , is neglected because at microwave frequencies the current flow in the lateral wires is concentrated at the outer surface. This excitation is forced to be one of the boundary values of equation (1). Applying the Fourier equation to the boundary gives the power at the surface[4]

$$q = -\oiint_S k(\nabla T)\cdot\bar{n}\, d\sigma \tag{2}$$

where $q$ = heat flow rate

$k$ = thermal conductivity

$T$ = temperature

$\bar{n}$ = surface normal vector

$\sigma$ = area

$S$ = surface

$\nabla$ = gradient

The initial condition, the value of temperature at time equal to zero, is the steady state temperature before the pulse r.f. grid excitation starts. This value is assumed

$$T_o = 350^{\circ}C \tag{3}$$

These equations describe a linear inhomogeneous initial-boundary value problem. A solution is - temperature T (t,z) that is a function of time and position that reduces equation (1) to an identity and also describes the assumed boundary conditions (2) and satisfies the initial condition (3) at time zero.

These equations are solved using three different boundary conditions as follows:

Case I. Constant heat flux, F, applied to the surface of the lateral wire at time zero and the wire not connected to a heat sink.

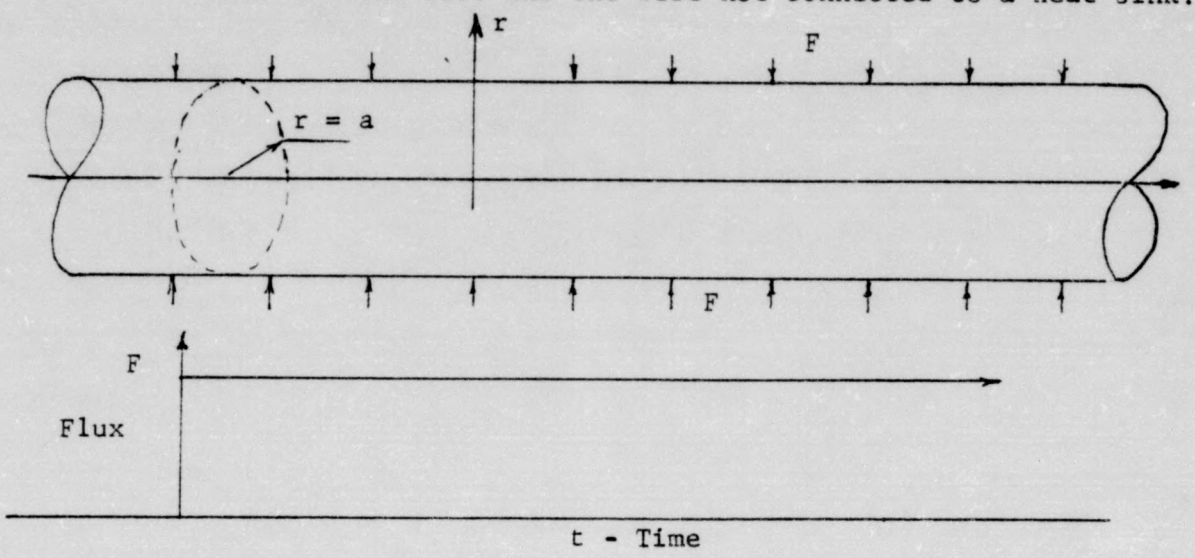


Case II. The same as Case I except the ends of the lateral wires, of length L, are connected to a heat sink (the grid frame) at temperature $T_f$.

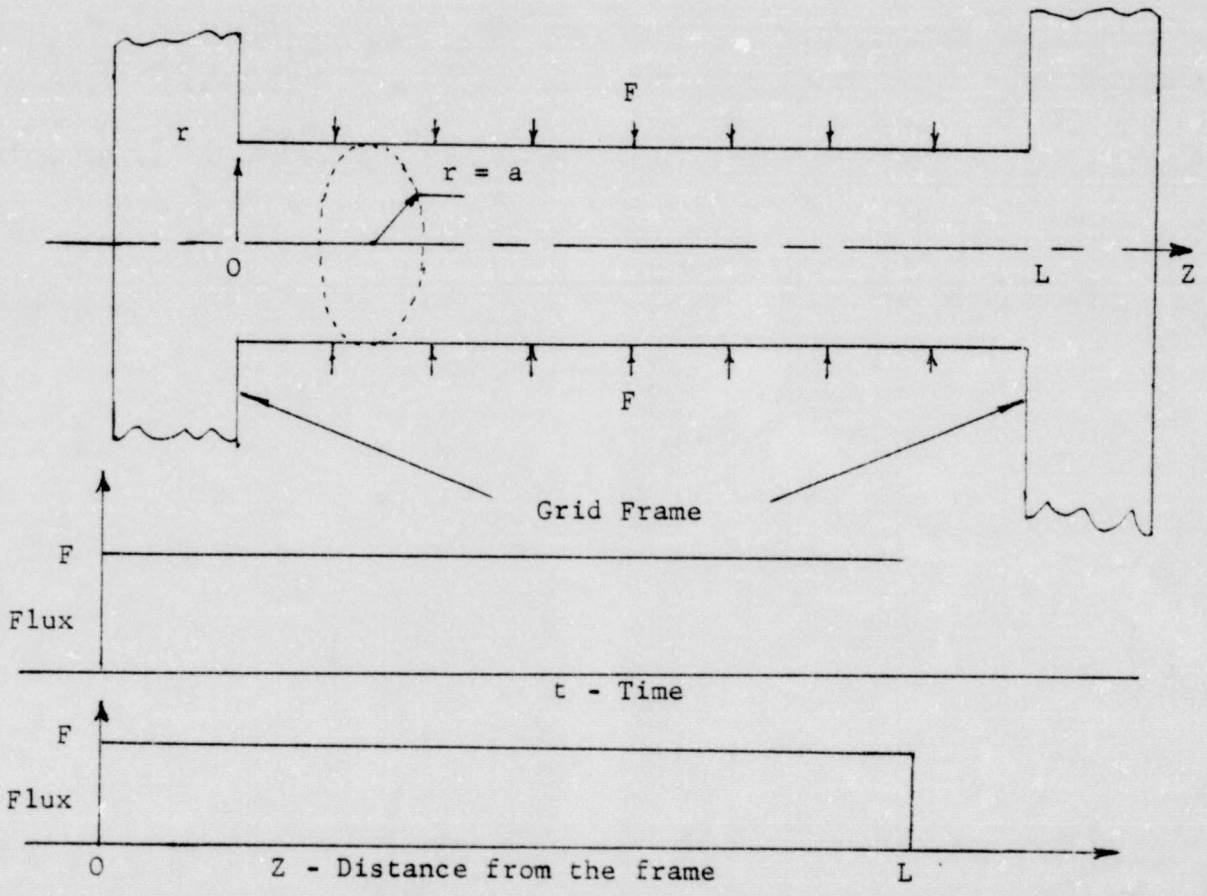

Case III. In this case the heat flux, F, is applied to the surface of the lateral wire in the form of pulses occurring for $\tau$ seconds, off for $T-\tau$ seconds, repeating at intervals of T seconds. The ends of the lateral wires are connected to a heat sink (the grid frame) at temperature $T_f$, assumed to be 350°C.

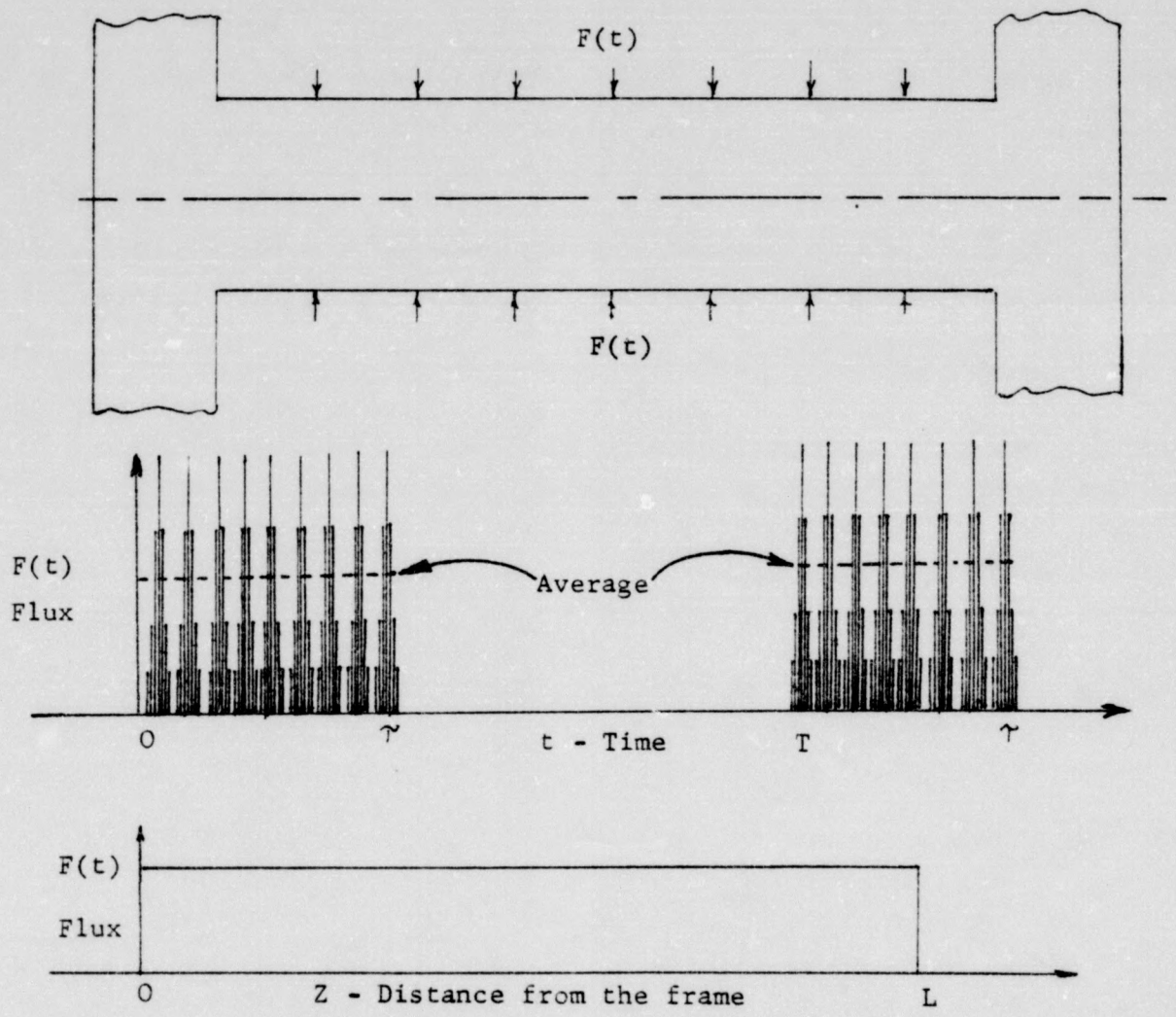


These three different boundary conditions are applied to the basic equations, pp 10 and 11, and the derivations are given for Case I, Case II, and Case III in appendixes A, B, and C, respectively. The solutions from appendixes A, B, and C are given in Chapter III.

The heat flux, F, or power dissipated in the grid per unit area, is in the form of pulses as shown in Figure 5, page 7. This grid excitation is approximated by assuming the average flux is applied to the grid for $\tau$ seconds. The input data is usually a wattmeter reading which can be converted to a flux for $\tau$ seconds by knowing the excitation duty cycle (percent time on) and the frequency of the pulses (repetition rate).

# CHAPTER III

## SOLUTIONS TO THE INITIAL-BOUNDARY VALUE PROBLEM

### Definitions of Variables and Constants

$r$ = variable distance from the center of grid wire.

$a$ = radius of grid wire.

$z$ = variable distance from the grid frame.

$L$ = length of lateral wire.

$t$ = time.

$T(r,t)$ = temperature of grid lateral wire as a function of r and t.

$T(z,r,t)$ = temperature of grid lateral wire as a function of z, r, and t.

$T_o$ = steady state temperature before applied grid excitation.

$F$ = constant heat flux.

$F(t)$ = heat flux as a function of time.

$k$ = conductivity of the grid wire.

$\alpha$ = thermal diffusivity of the grid wire.

$A$ = surface area of the grid lateral wire.

$\lambda n$ = positive roots of $J_1(\lambda n) = 0$.

$J_n$ = Bessel function order n.

$I_n$ = modified Bessel function order n.

Assuming the grid wire excitation does not depend on the angle; i.e., the heat flux on the lateral surface area is uniform, equations (1), (2), and (3) pp.10 and 11 are as follows in cylindrical coordinates,

(4) $$\frac{1}{\alpha}\frac{\partial T(r,z,t)}{\partial t} = \frac{1}{r}\frac{\partial}{\partial r}\, r\,\frac{\partial T(r,z,t)}{\partial r} + \frac{\partial^2 T}{\partial z^2}(r,z,t) + \frac{1}{r^2}\frac{\partial^2 T}{\partial \theta^2}(r,z,t)$$ $= 0$

Between the limits of: $0 \leq r \leq a$, $0 \leq z \leq L$, $t > 0$

and at the boundary (surface of the wire),

(5) $$F = \frac{q}{A} = -k\,\frac{\partial T}{\partial r}(r,z,t)$$

Between the limits of: $r = a$, $0 < z < L$, $t > 0$

Another boundary condition that must be used if the grid lateral wire is connected to a frame is,

$$T(\text{wire}) \text{ or } T(r,z,t) = T(\text{frame}) \quad \text{at } z = 0 \text{ and } L$$

In this analysis, the T(frame) is assumed to be 350°C

and the initial condition,

(6) $$T(r,z,t) = 350^{\circ}C$$

Between the limits of: $0 \leq r \leq a$, $0 \leq z \leq L$, $t = 0$

These equations applied to Case I, Case II, and Case III give the following solutions:

Case I Constant heat flux, F, applied to a long wire at t = 0, wire not connected to a frame.

$$\frac{1}{\alpha}\frac{\partial T(r,t)}{\partial t} = \frac{1}{r}\frac{\partial}{\partial r}\, r\,\frac{\partial T(r,t)}{\partial r} \qquad \begin{matrix} 0 \leq r \leq a \\ t > 0 \end{matrix} \tag{7}$$

Boundary condition:

$$F = \frac{q}{A} = -k\,\frac{\partial T(r,t)}{\partial r} \qquad \begin{matrix} r = a \\ t > 0 \end{matrix} \tag{8}$$

Initial condition:

$$T(r,t) = 350^{\circ}C \qquad \begin{matrix} 0 \leq r \leq a \\ t = 0 \end{matrix} \tag{9}$$

Solution:

$$T(r,t) = T(r,o) + \frac{Fa}{k}\left[\frac{2\alpha t}{a^2} + \frac{r^2}{2a^2} - \frac{1}{4} - 2\sum_{n=1}^{\infty} e^{-\frac{\alpha \lambda_n^2 t}{a^2}}\,\frac{J_o(\lambda_n^2 \frac{r}{a})}{\lambda_n^2 J_o(\lambda_n)}\right] \tag{10}$$

where $\lambda_n$ are the positive roots of $J_1(\lambda_n) = 0$

See appendix A for the complete solution

The solution to this problem is found in Conduction of Heat in Solids by H.S. Carslaw and J.C. Jaeger, 2nd edition, pp. 328 and 329.

Case II Constant heat flux, F, applied to the surface of the lateral wire at t = 0 and the wire connected to a heat sink at the ends, z = 0 & L.

$$\frac{1}{\alpha}\frac{\partial T}{\partial t}(r,z,t) = \frac{1}{r}\frac{\partial}{\partial r}\left[r\frac{\partial T}{\partial r}(r,z,t)\right] + \frac{\partial^2 T}{\partial z^2}(r,z,t) \qquad \begin{array}{l} 0 \le r \le a \\ 0 \le z \le L \\ t > 0 \end{array} \tag{11}$$

Boundary condition:

$$F = \frac{q}{A} = -k\frac{\partial T}{\partial r}(r,z,t) \qquad \begin{array}{l} r = a \\ 0 < z < L \\ t > 0 \end{array}$$

$$T(r,0,t) = T(r,L,t) = 350^{\circ}C \qquad \begin{array}{l} 0 \le r \le a \\ 0 \le z \le L \\ t = 0 \end{array} \tag{12}$$

Initial condition:

$$T(r,z,0) = 350^{\circ}C \qquad \begin{array}{l} 0 \le r \le a \\ 0 < r < L \\ t = 0 \end{array} \tag{13}$$

Solution: <u>See appendix B for the complete solution</u>

$$T(r,z,t) = T(r,z,0) + \sum_{n=1,3}^{\infty} \frac{4F\sin(\rho z)}{n\pi k}\left\{S_1 - S_2 - S_3\right\} \tag{14}$$

where

$$S_1 = \frac{I_0(\rho r)}{\rho I_1(\rho a)}$$

$$S_2 = \frac{2\,e^{-\alpha\rho^2 t}}{a\,\rho^2}$$

$$S_3 = \sum_{m=1,2,3\cdots}^{\infty} \frac{2\,J_0\left(\lambda_m \frac{r}{a}\right)e^{-\alpha\left(\frac{\lambda_m^2}{a^2}+\rho^2\right)t}}{a\,J_0(\lambda_m)\left\{\frac{\lambda_m^2}{a^2}+\rho^2\right\}}$$

$$\rho = \frac{n\pi}{L}$$

Case III The grid drive excitation is in the form of pluses, on $\tau$ seconds, off T - $\tau$ seconds, repeating at T seconds. The wire is heat sinked and is equal to the frame temperature at z = 0 and L.

$$\frac{1}{\alpha}\frac{\partial T(r,z,t)}{\partial t} = \frac{1}{r}\frac{\partial}{\partial r}\, r\,\frac{\partial T(r,z,t)}{\partial r} + \frac{\partial^2 T(r,z,t)}{\partial z^2} \qquad \begin{matrix} 0 \le r \le a \\ 0 \le z \le L \\ t > 0 \end{matrix} \tag{15}$$

Boundary conditions:

$$F(t) = \frac{q}{A} = -k\,\frac{\partial T(r,z,t)}{\partial r} \qquad \begin{matrix} r = a \\ 0 < z < L \\ t > 0 \end{matrix} \tag{16}$$

where F(t) is on $\tau$ seconds and off T- $\tau$ seconds as follows:

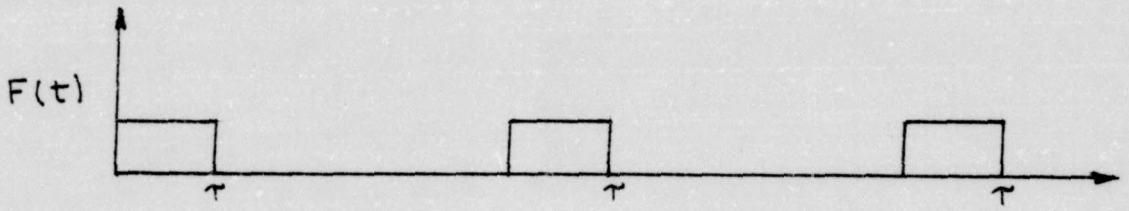


$$\text{and,}\quad T(r,o,t) = T(r,L,t) = 350^{\circ}C \qquad \begin{matrix} 0 \le r \le a \\ 0 \le z \le L \\ t = 0 \end{matrix} \tag{17}$$

Initial condition:

$$T(r,z,0) = 350^{\circ}C \qquad \begin{matrix} 0 \le r \le a \\ 0 \le z \le L \\ t = 0 \end{matrix} \tag{18}$$

Solution:

This solution was developed using the Dirac function[5] and the convolution integral[6] after LaPlace and Fourier transforms.[7]

The solution is not in closed form and the temperature must be calculated starting at t = 0 and summed as a function of time. The solution for one pulse is:

(19)

$$T(r,z,t) = T(r,z,0) + F\sum_{n=1,3}^{\infty} K_n \left\{ S_4 + \sum_{m=1,2,3}^{\infty} K_m S_5 - S_6 - \sum_{m=1,2,3}^{\infty} K_m S_7 \right\}$$

where $$p_n = \frac{n\pi}{L}$$

$$K_n = \frac{8\alpha \sin(p_n z)}{n\pi k a}$$

$$K_m = \frac{J_0(\lambda_n \frac{r}{a})}{J_0(\lambda_n)}$$

$$S_4 = \frac{1 - e^{-\alpha p_n^2 t}}{\alpha p_n^2}$$

$$S_5 = \frac{1 - e^{-\alpha\left[\frac{\lambda_n^2}{a^2} + p_n^2\right] t}}{\alpha\left[\frac{\lambda_n^2}{a^2} + p_n^2\right]}$$

$$S_6' = \frac{1 - e^{-\alpha p_n^2 (t-\tau)}}{\alpha p_n^2}$$

$$S_7' = \frac{1 - e^{-\alpha\left[\frac{\lambda_n^2}{a^2} + p_n^2\right](t-\tau)}}{\alpha\left[\frac{\lambda_n^2}{a^2} + p_n^2\right]}$$

Figure 7, page 22, is a graph of the calculated grid lateral wire temperature of the ceramic triode type GE18651, for Case I, II, and III. The temperature for Case III is a function of the % duty (percent of time the excitation is applied for one cycle). When the pulse is on 100% of the time, Case III is then the same as Case II.

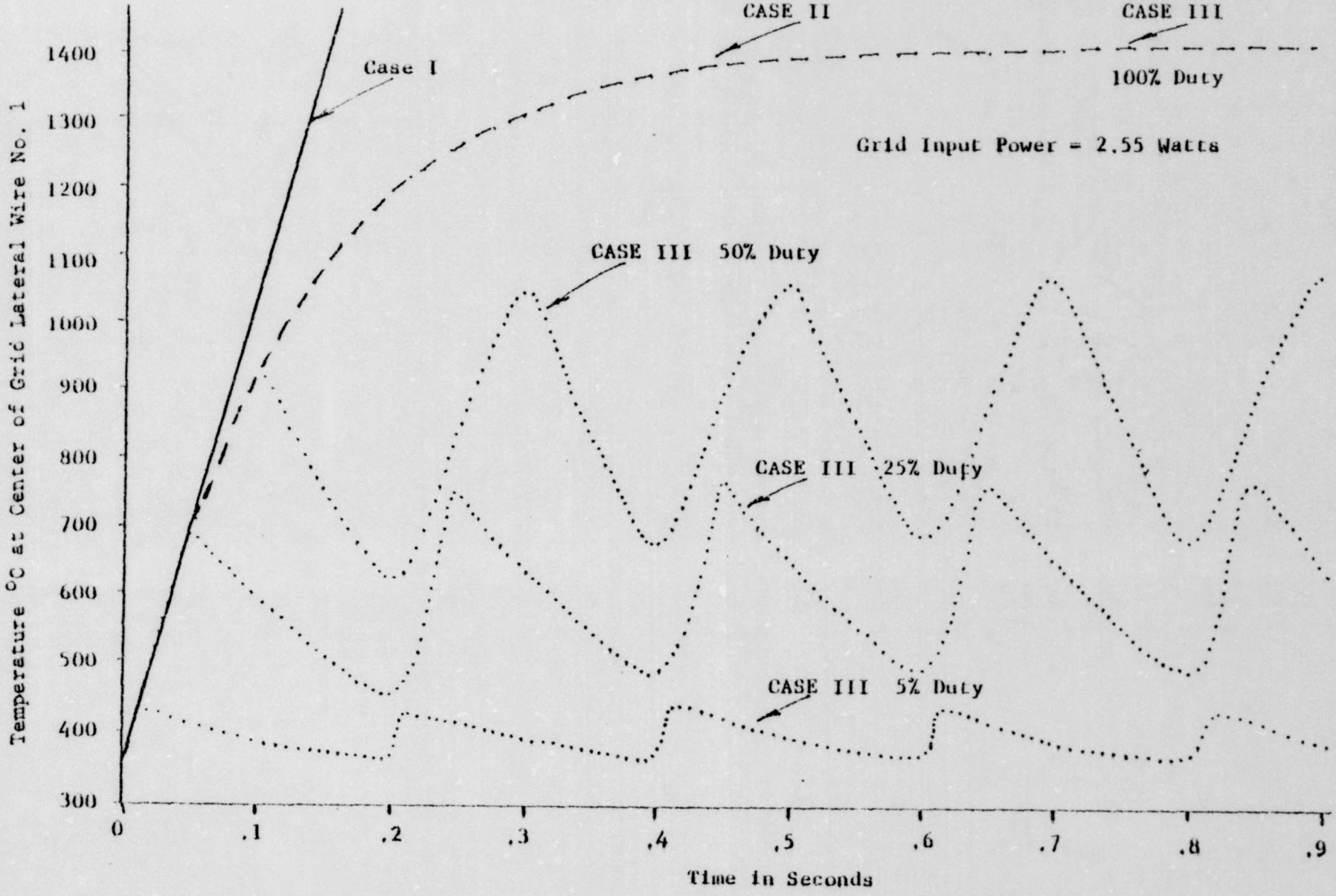


Figure 7 - GE18651 Grid Lateral Temperature for Case I, Case II, and Case III at 100, 50, 25, and 5% Duty Cycles

# CHAPTER IV

## CALCULATED LATERAL WIRE TEMPERATURE AS A FUNCTION OF SEVERAL VARIABLES

The temperature of a grid lateral wire is a function of several variables that are related to the grid excitation, the dimensions of the grid wire, and the physical material characteristics.

This analysis neglects the effect of variations in the grid frame temperature, the radiation from the grid laterals, and assumes a temperature of 350°C before the grid excitation is applied.

The grid used in the ceramic planar power triode GE18651 (see Figure 5(a), p. 7) was used to calculate the temperature of the grid lateral wire.

The GE18651 grid has the following excitation, dimensions, and physical characteristics:

A. Excitation

1. Input power, q = 2.55 watts
2. Repetition rate, T = .2 seconds
3. % Duty cycle, 50% ($\tau$ = .1 second)

B. Dimensions

4. Lateral wire diameter, d = .0006" (.001524 cm)
5. Length, turn No. 1, = .300" = .762 cm
   10 = .296" = .752 cm
   20 = .284" = .7218 cm
   30 = .263" = .6681 cm
   40 = .230" = .584 cm
   50 = .183" = .45591 cm
   60 = .0882" = .209348 cm
   62 = .034" = .086 cm

B. Dimensions (Cont'd)

6. Turns per inch, TPI = 416

7. Total turns, TT = 124

C. Physical Material Characteristics

8. Material, Tungsten

9. Thermal conductivity, $k = .300 \ \frac{Cal}{sec.-{}^{o}C-cm}$

10. Mass density, $m = 19.3 \ \frac{gm}{cm^3}$

11. Specific heat, $Cp = .033 \ \frac{Cal}{gm-{}^{o}C}$

12. Diffusivity, $\alpha = \frac{k}{mCp} = .471 \ \frac{cm^2}{sec.}$

D. Temperatures are at the center of the wire and frame.

Using the above constrains as the control, the temperature of the GE18651 grid lateral is investigated by varying each of the above characteristics.

GE18651 Grid Temperature

Figure 8 - excitation 5.1, 2.55, and 1.27 watts.

Figure 9 - repetition rate of .1, .2, and .4 second.

Figure 10 - pulse on time ( $\tau$ ) varied from .01 to .2 second.

Figure 11 - of turns No. 1, No. 43, No. 54, and No. 62 as a function of length from the frame.

Figure 12 - lateral wire diameter of .0004", .0006", and .0008".

Figure 13 - at center of the wire mid-span for turns No. 1, No. 2 .... 62.

Figure 14 - grid wire material changed to titanium and gold.

| | k Thermal Conductivity | $\alpha$ Diffusivity |
|---|---|---|
| Tungsten | .3 | .471 |
| Titanium | .033 | .0495 |
| Gold | .7 | 1.067 |

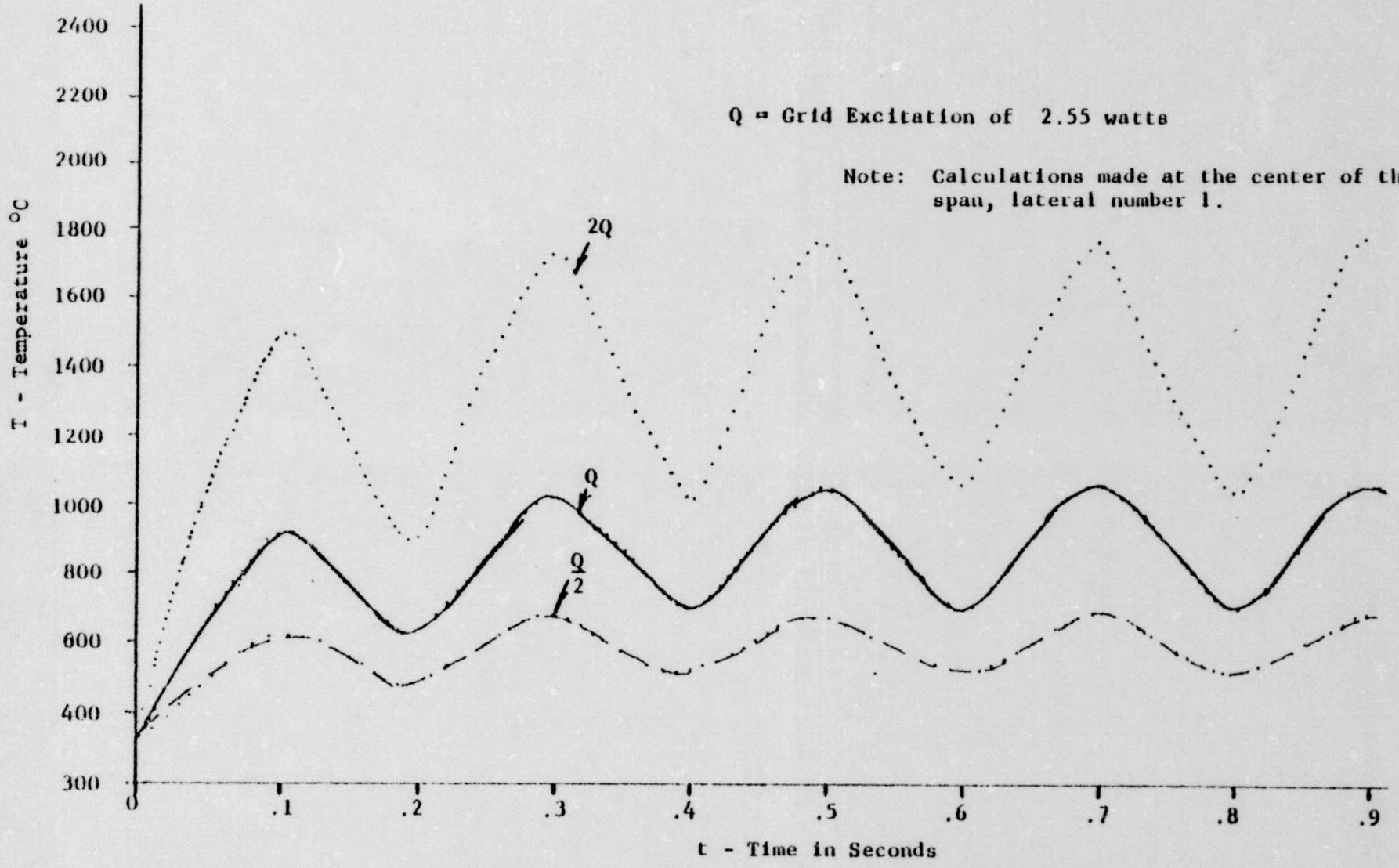


Figure 8 - GE18651 grid lateral temperature at three input excitations.

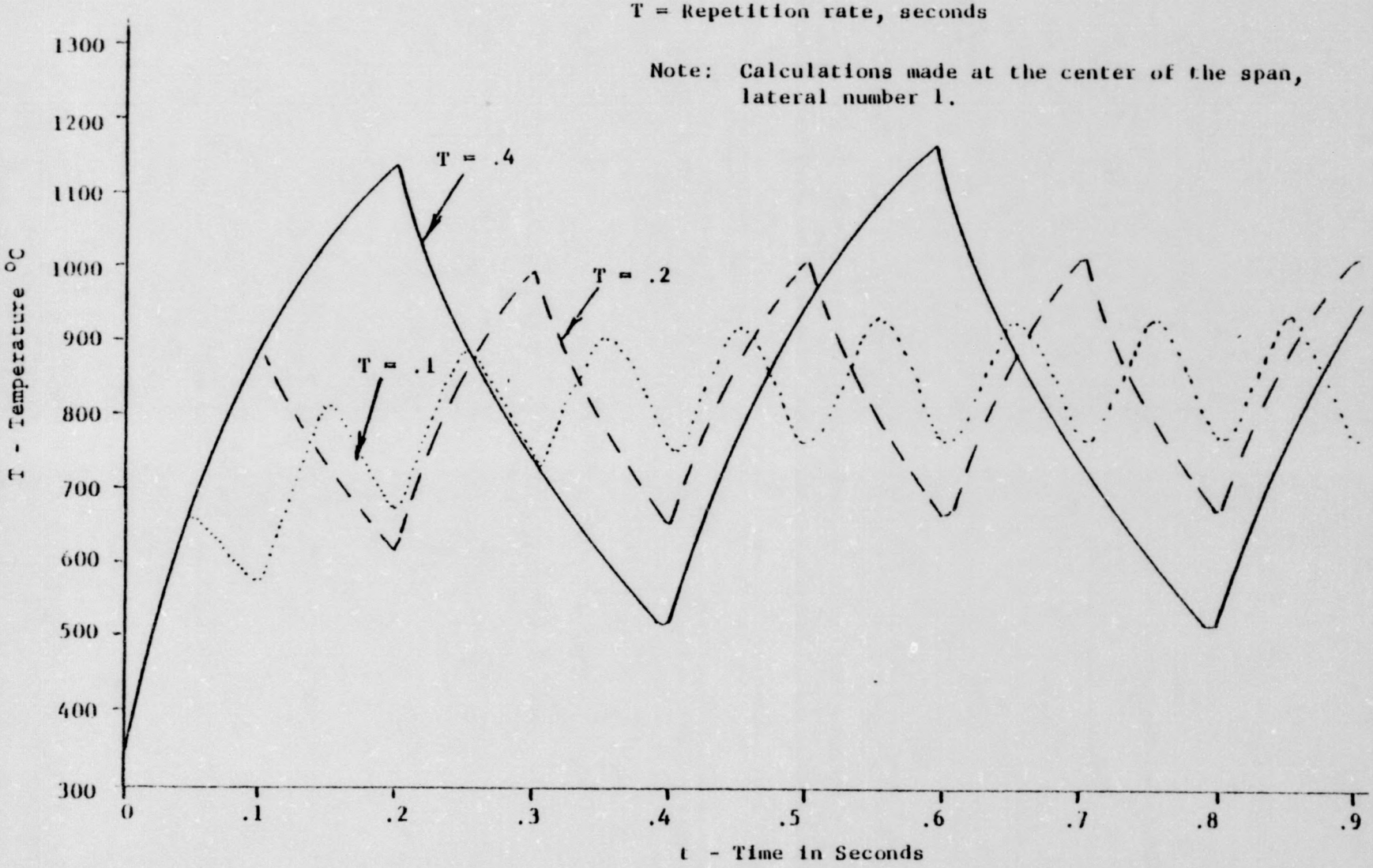


Figure 9 - GE18651 Grid Lateral Temperature at Three Repetition Rates

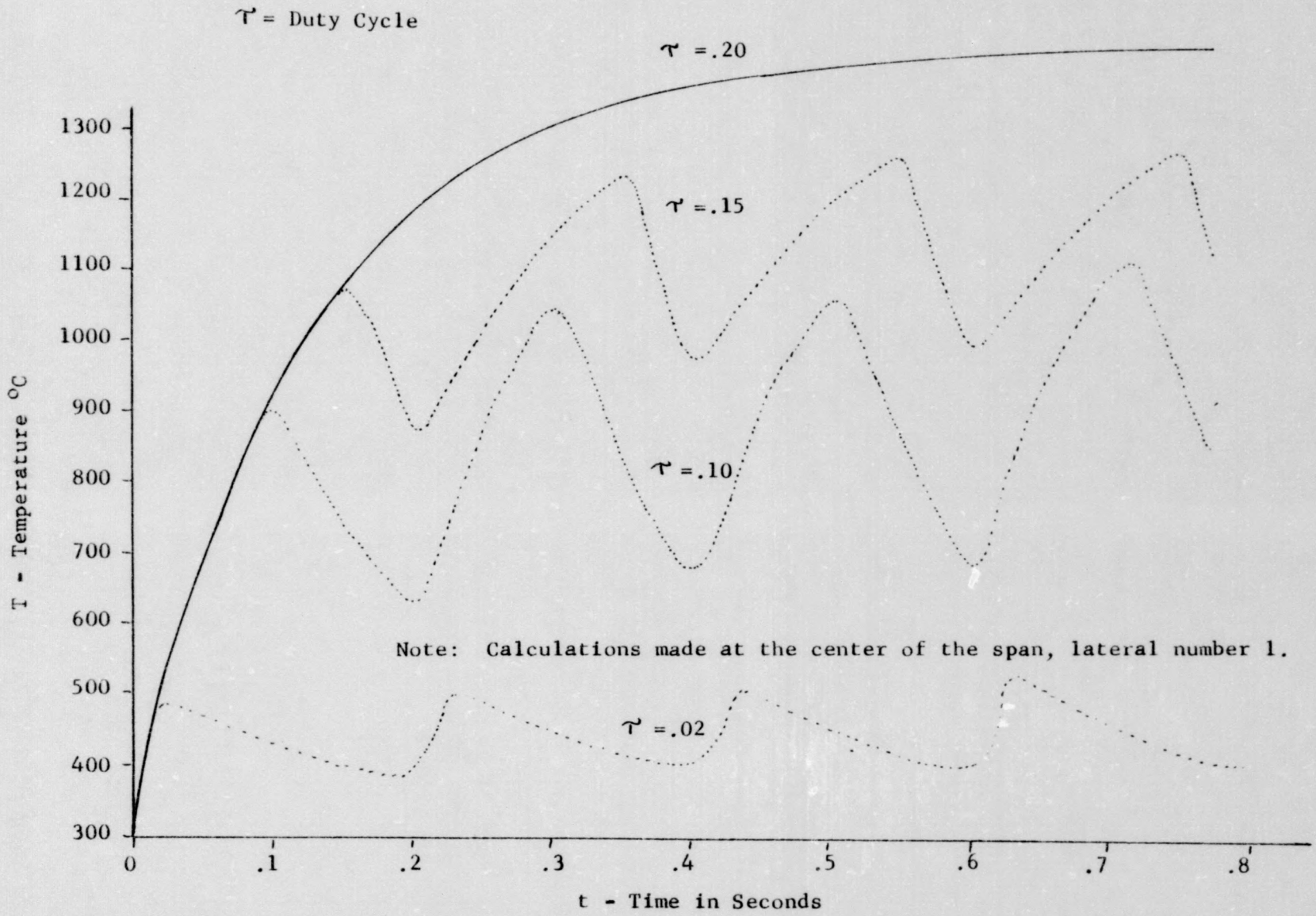


Note: Calculations made at the center of the span, lateral number 1.

Figure 10 - GE18651 Grid Lateral Temperature as a Function of Duty Cycle

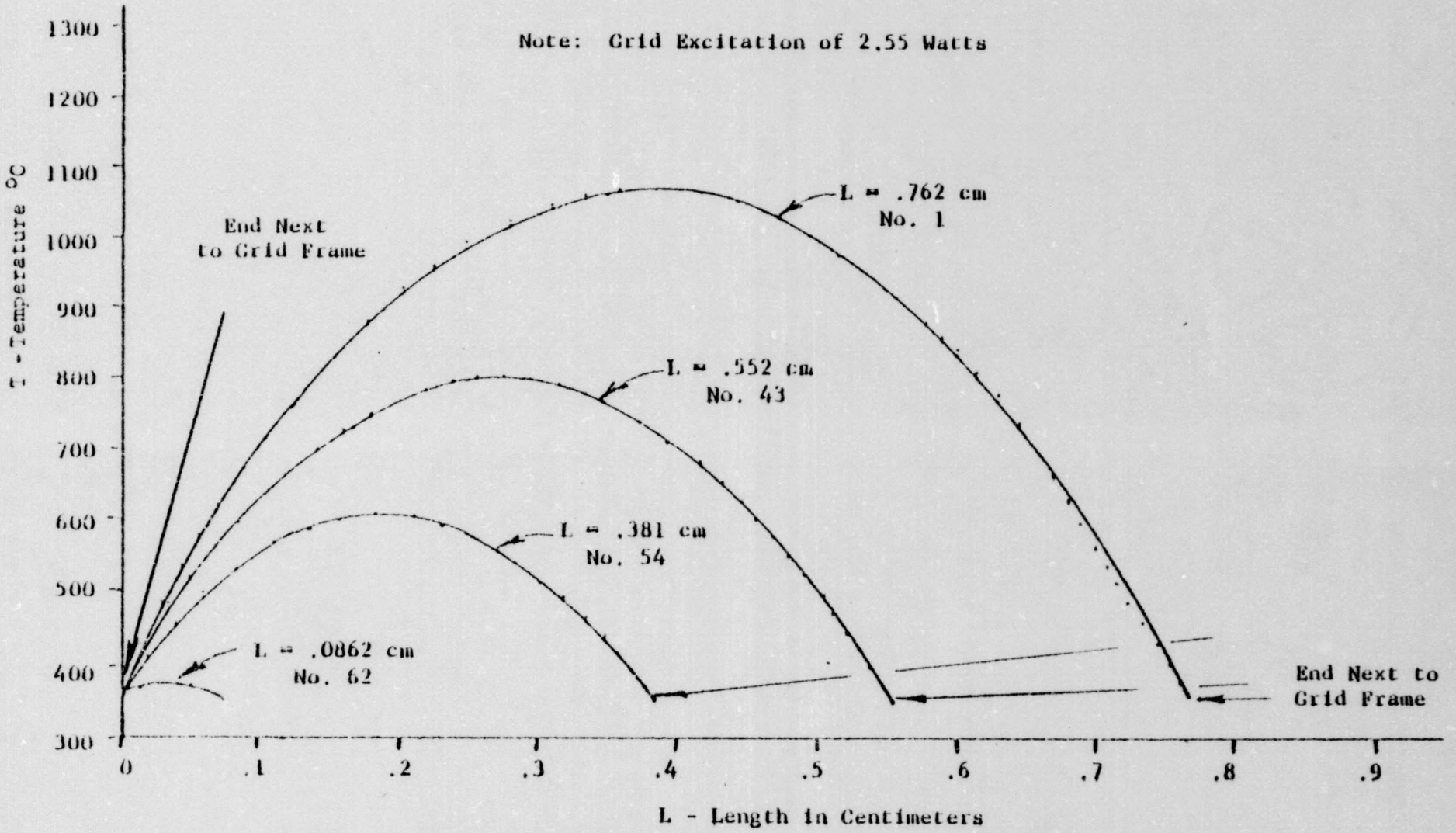


Figure 11 - GE18651 Grid Lateral Temperature for Three Different Length Lateral Wires

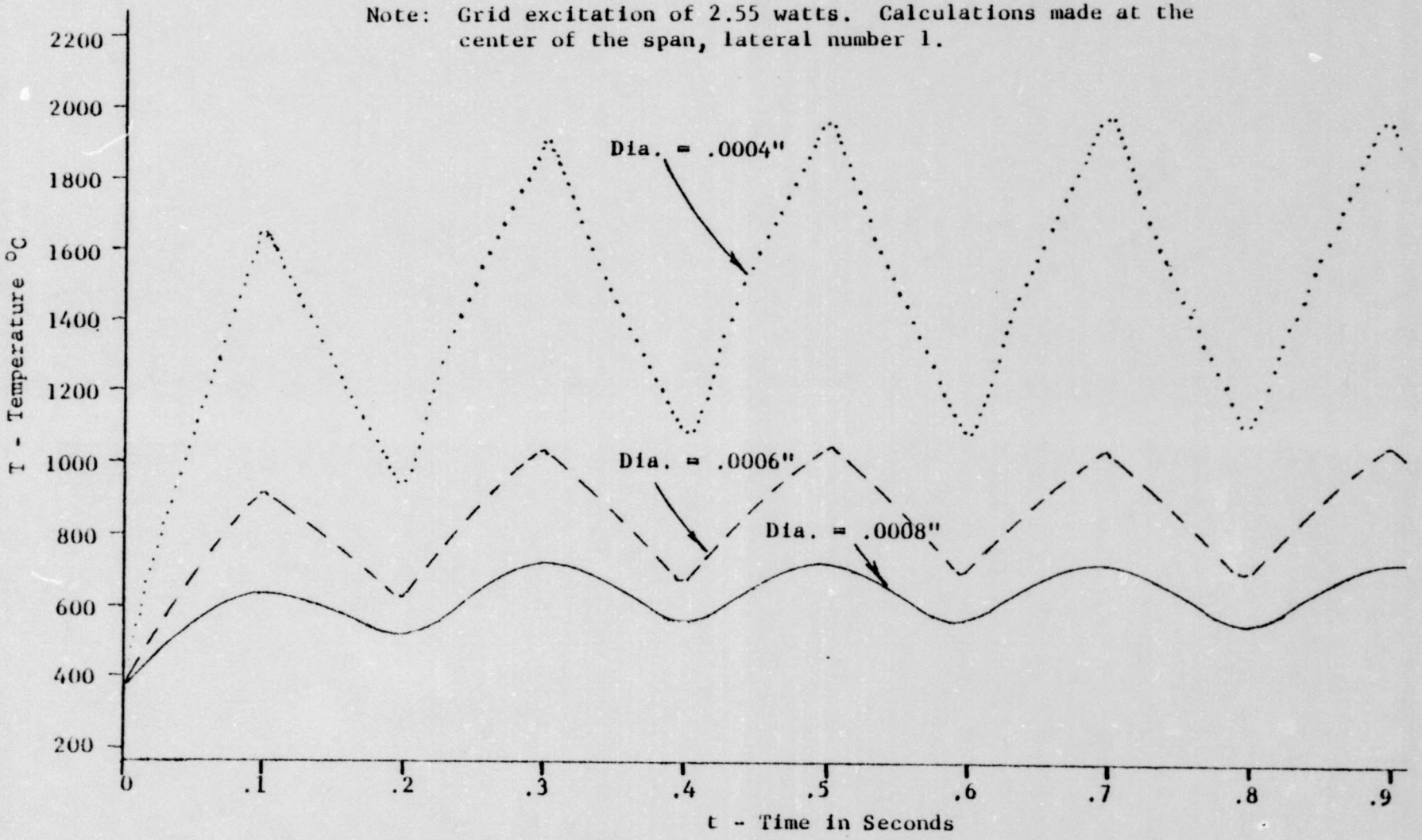


Figure 12 - GE 18651 Grid Lateral Temperature for Three Wire Diameters

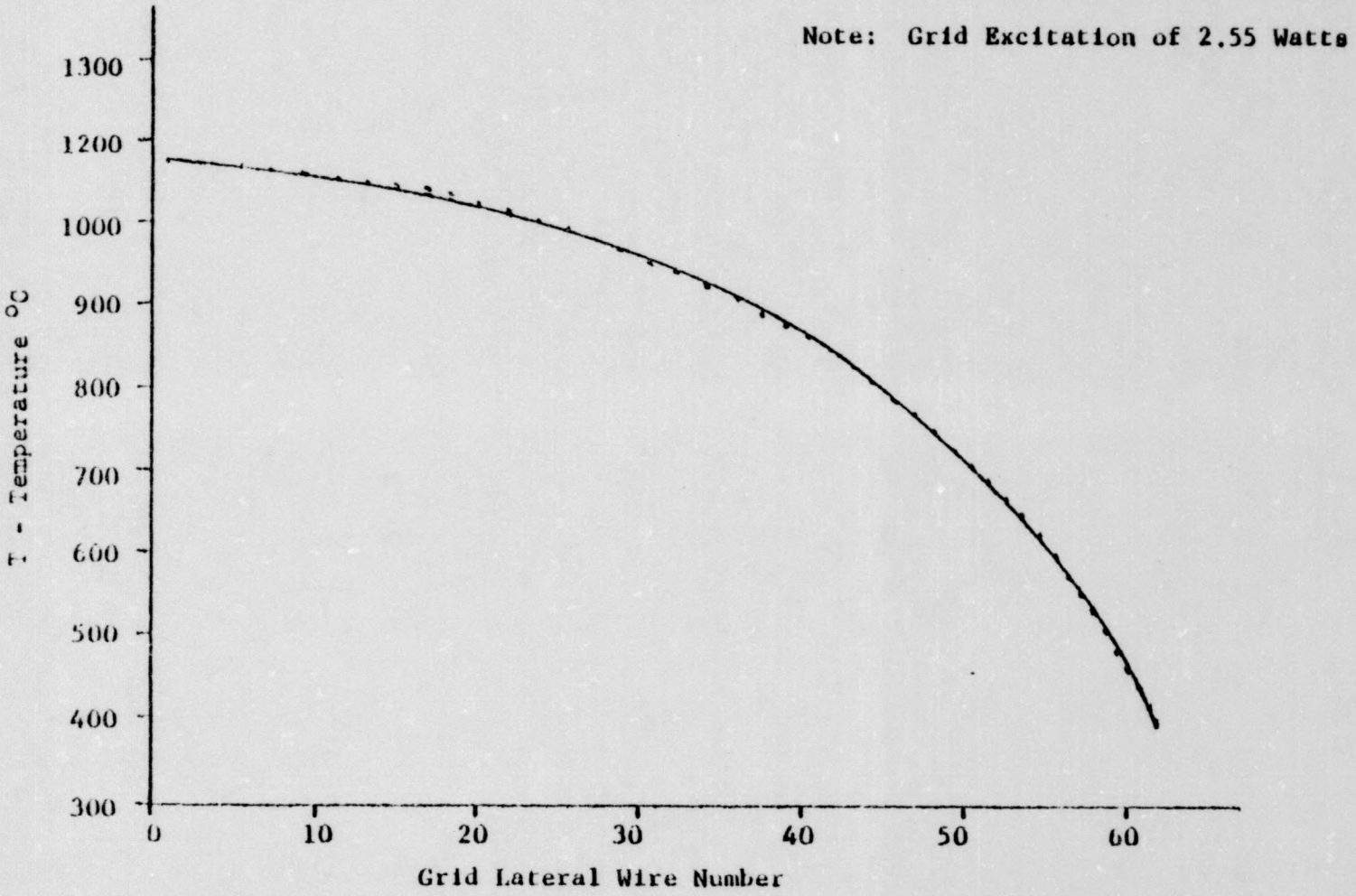


Figure 13 - GE 18651 Center of Grid Temperature from 1st to 62nd.

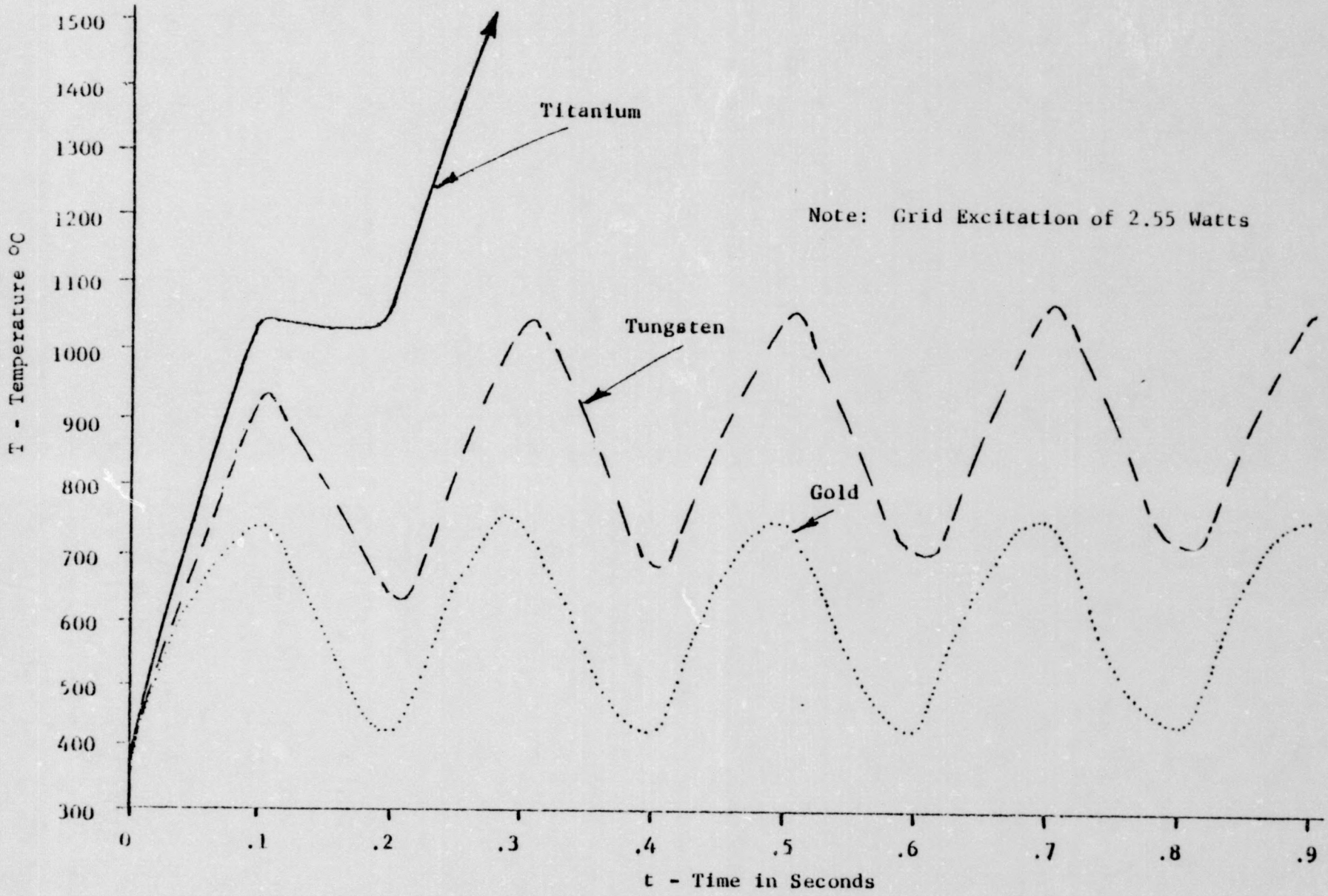


Figure 14 - GE18651 Grid Lateral Temperature for Three Different Wire Materials

# CHAPTER V

# EXPERIMENTAL VERIFICATION

The principal reason for choosing this particular subject for investigation was that the performance and reliability of microwave power triodes are related to grid drive power. This grid excitation causes lateral wire heating and the grid lateral wire temperatures cannot be measured by thermocouples or optical pyrometers.

This reason suggests that a tube experiment is not a candidate for an accurate experimental verification of the derived equations. However, since tube grid temperature information was the motivation for this development, the experiments are in two parts:

1. Constant boundary conditions to verify the derived equations.
2. Tube boundary conditions to establish the significance of these equations in tube design or application problems.

## Constant Boundary Conditions Experiment

The lateral surface area of a copper rod was excited with heat flux in a vacuum. The outer surface was covered with aluminum foil and asbestos insulating tape to reduce the surface radiation. The ends of the rod were connected to a constant temperature heat sink and the temperature of the rod was measured as a function of time. Figure 15 is a drawing showing a top and cross sectional view of the experiment and page 34 is a photograph.

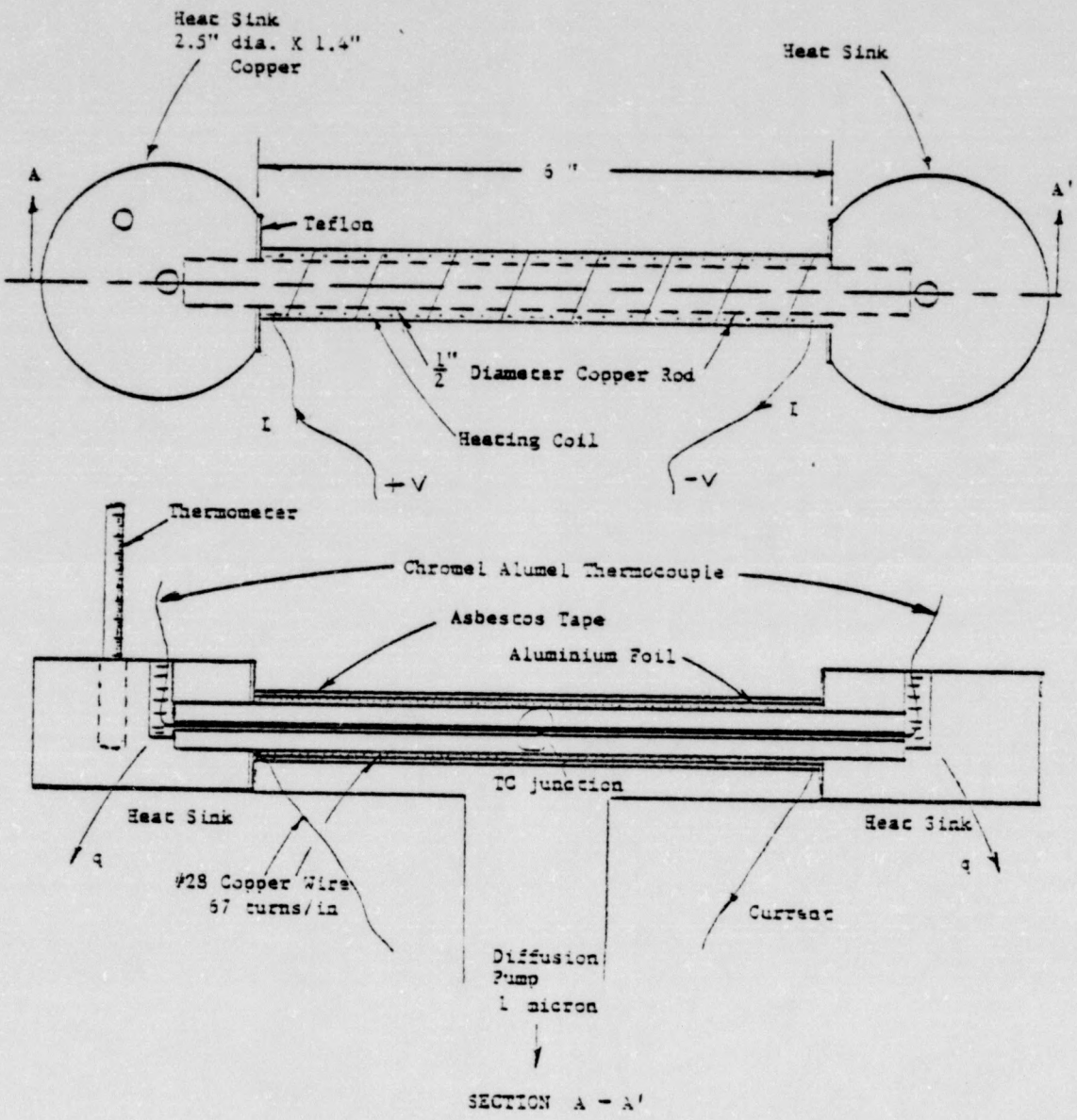


Figure 15 — Lateral Surface Area of Copper Rod Heated in a Vacuum

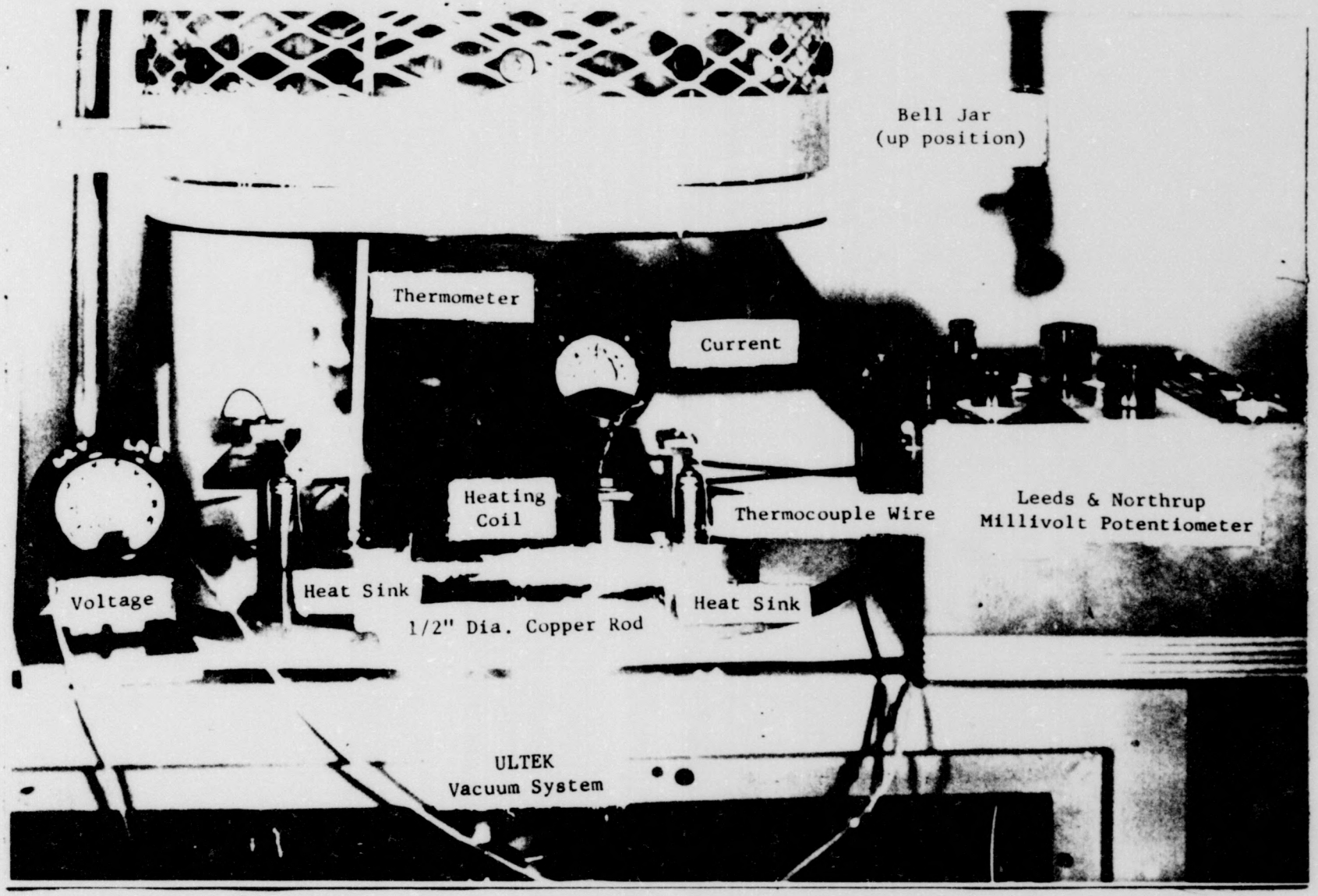


I - Photograph of Experimental Apparatus Used to Heat the Surface of a Copper Rod and Measure Temperature as a Function of Time

Figure 16 shows a plot of the calculated temperatures compared to the measured temperatures for four surface excitations.

## Microwave Tube Experiment

In the derivations, the heat sink temperature was assumed constant and the radiation from the anode and cathode surfaces was neglected. The lateral wire temperatures in a microwave triode are a function of these variables.

Microwave triodes, type GE18651, were used to determine the significance of the equations relative to actual lateral wire temperatures. The GE18651 grid is wound with .0006" tungsten wire, 416 turns per inch, 124 total turns across a .3" inside diameter frame. Tungsten melts at 3380°C. The computer program for the GE18651 grid lateral wire temperature, Appendix D, computes the grid temperature for grid drives equal to 6.25, 7.25, and 8.5 watts, Figure 17. These curves assume that the grid-cathode spacing is uniform, the cathode emission density does not vary across the surface of the cathode, neglects the radiation from the grid to anode and cathode, and does not include the heat of fusion of the melted turns.

Forty tubes, GE18651, were subjected to a ramp grid excitation until one or more turns opened because of tungsten melting. This was determined by monitoring the plate current cutoff, which is a sensitive test for windows in a grid.

Figure 18 is a distribution curve showing the grid power recorded when the cutoff current changed or grid lateral wires melted. The forty tubes were broken and the grids examined to determine the number of turns opened and location of the opened turns. This information is tabulated

in Appendix E. In most cases, when the grid power was low, an examination of the damaged grid wire revealed that turns opened because the grid shorted to the cathode rather than opened because of high temperature due to the grid drive power.

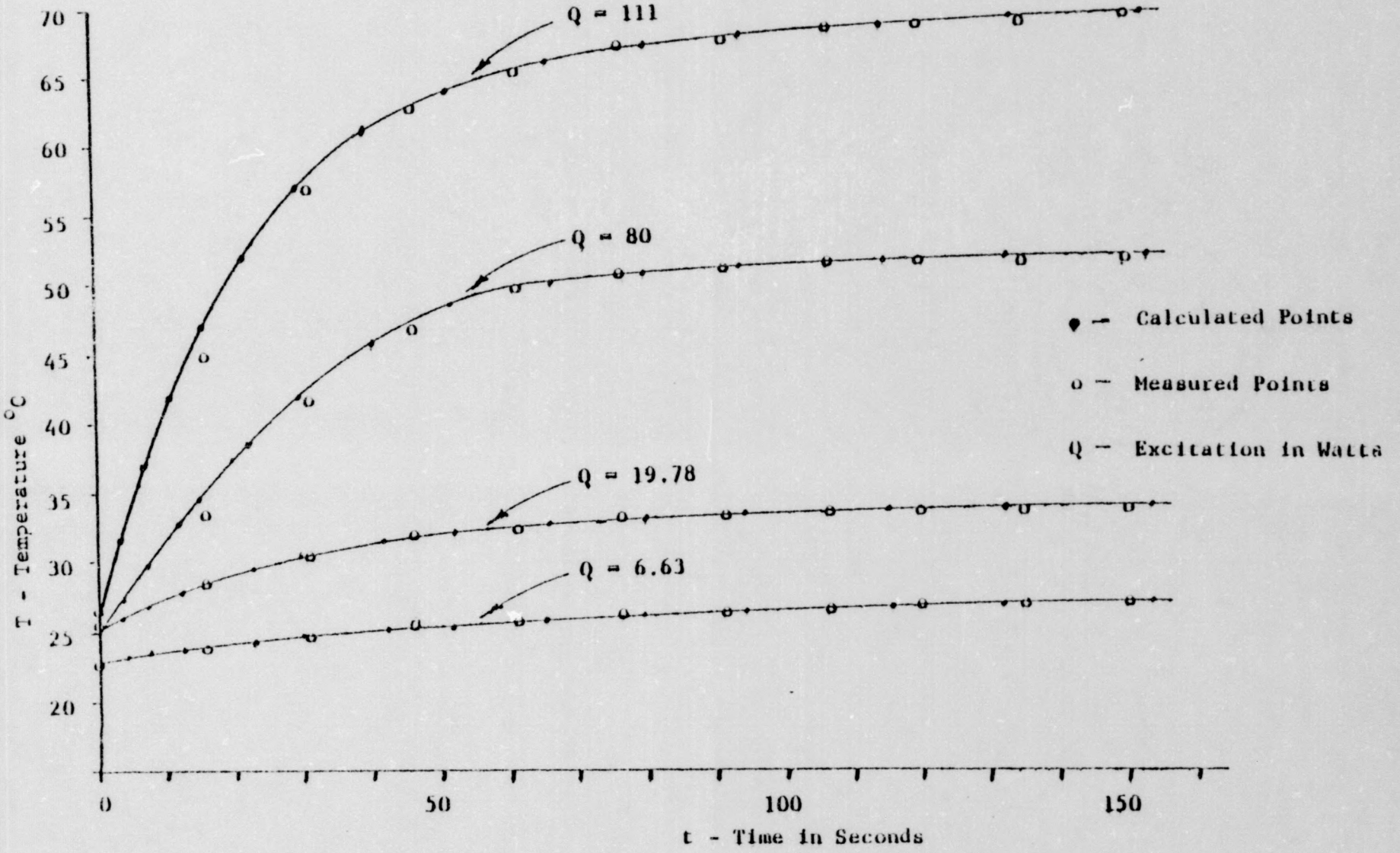


Figure 16 - Calculated Compared to Measured Temperatures when the Surface of a Copper Rod was Heated with Four Excitations

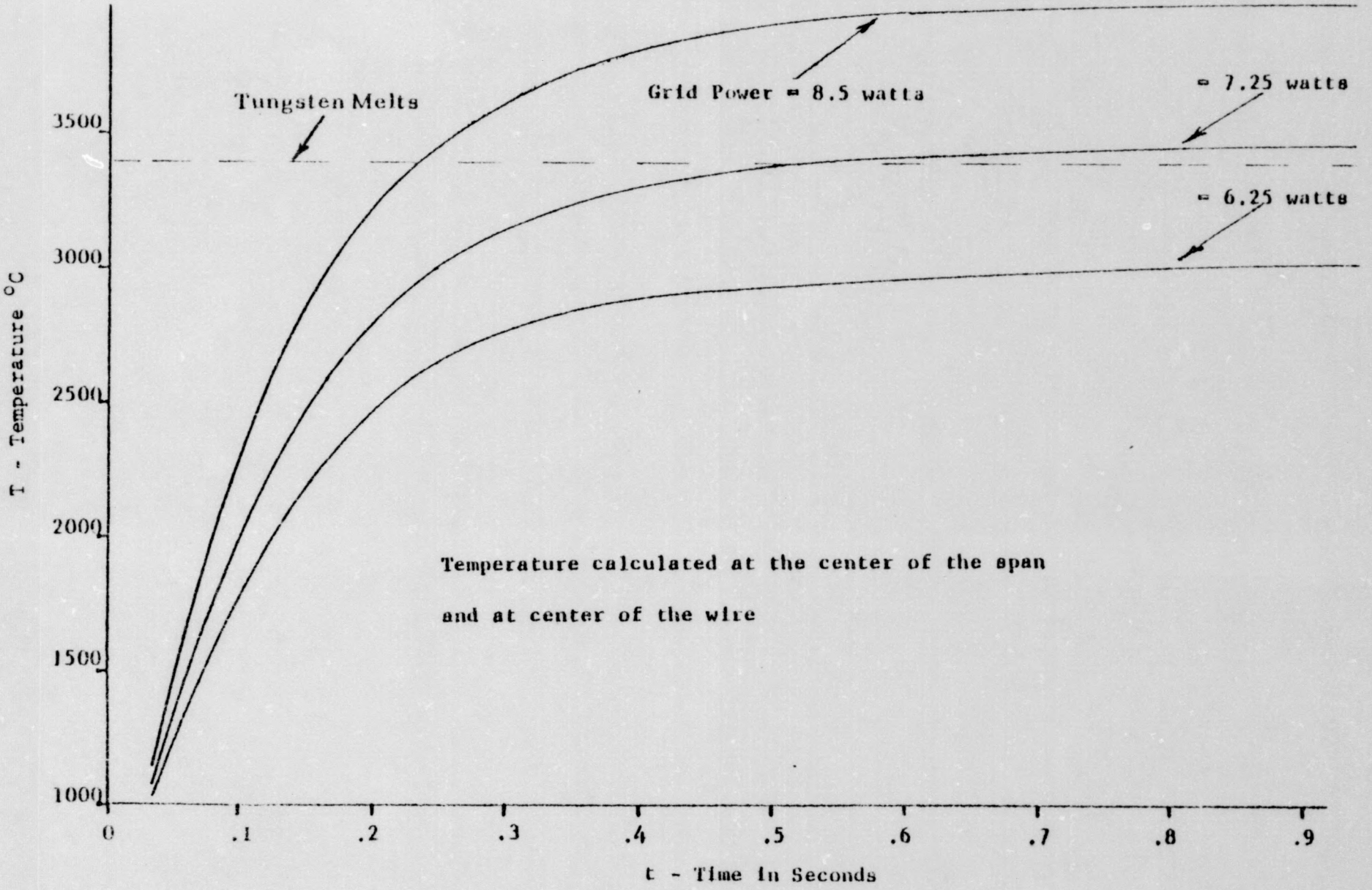


Figure 17 - Calculated Lateral Wire Temperature for Three Excitations

TUBE TYPE GE 18651
DISTRIBUTION OF Grid Power

TEST CONDITIONS:
Ef = 6.3 volts
If = 300 mA

Preheat:
Ep = 200 volts
Ip = 20 mA

Plate Current Cutoff
Ep = 200 volts
Eg = -7 volts

SAMPLE SIZE:
40 tubes

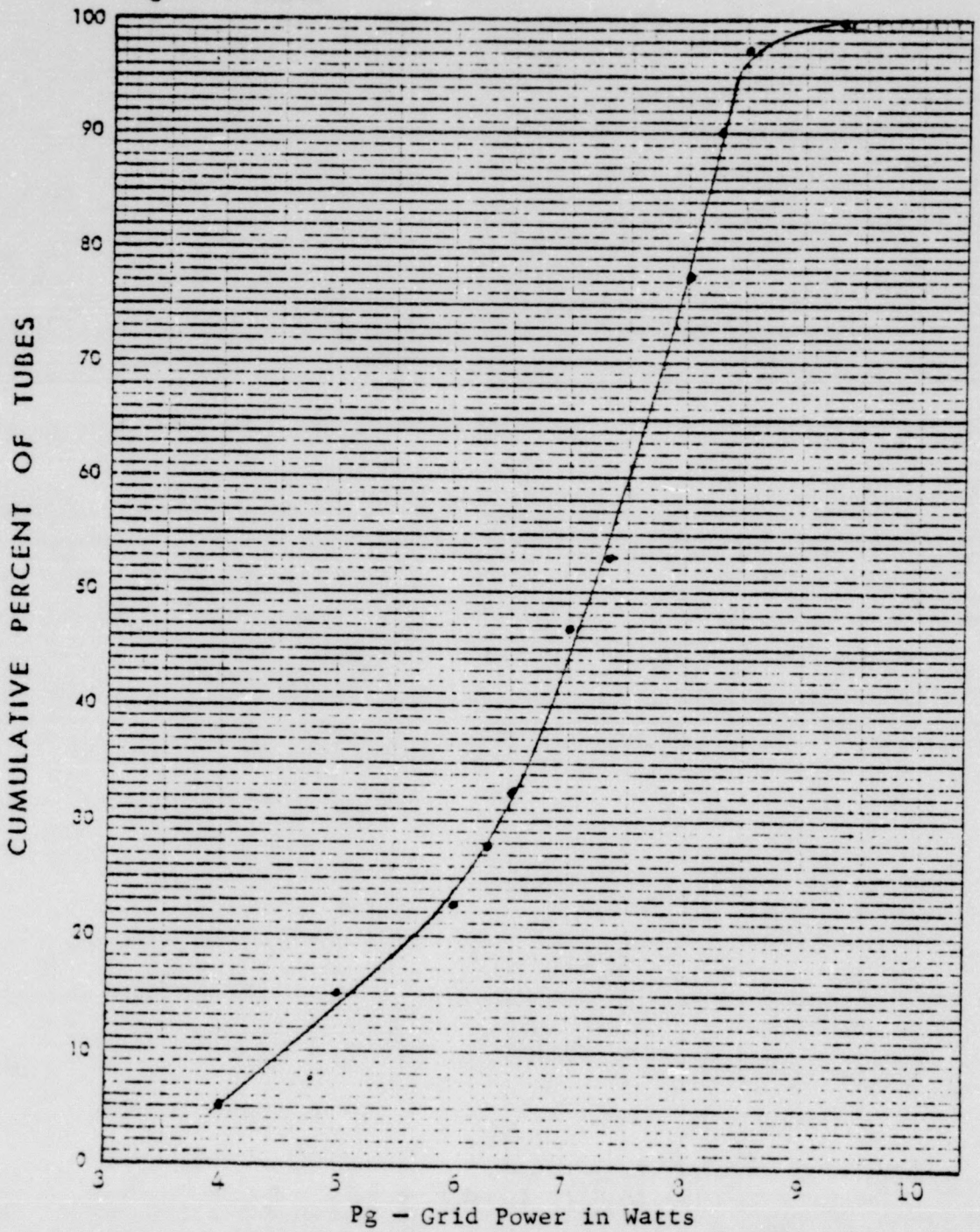


Figure 18 – Grid Excitation to Melt Tungsten Lateral Wire

# CHAPTER VI

# CONCLUSIONS

The general goal of this investigation was to develop equations that describe the temperature-time behavior of microwave power triodes grid lateral wires when subjected to pulses of grid power. An experiment confirms that the equations correctly calculate the temperature with the assumed boundary conditions. Another experiment, with aggravated boundary conditions sufficient to melt tungsten wire, indicates close agreement with the predicted calculated power.

Future work should be to calculate the anode and cathode temperatures. With these temperature profiles it seems reasonable that the grid heat sink temperature can be modeled and this could be used to iterate the lateral wire temperature solutions. The difficult task of including the radiation from cathode and anode surfaces is sufficient to discourage all but the highly motivated students of applied mathematics.

## APPENDIX A

Case I - Assume constant heat flux, F, is applied to the surface of a wire of infinite length, independent of θ at time equal to zero.

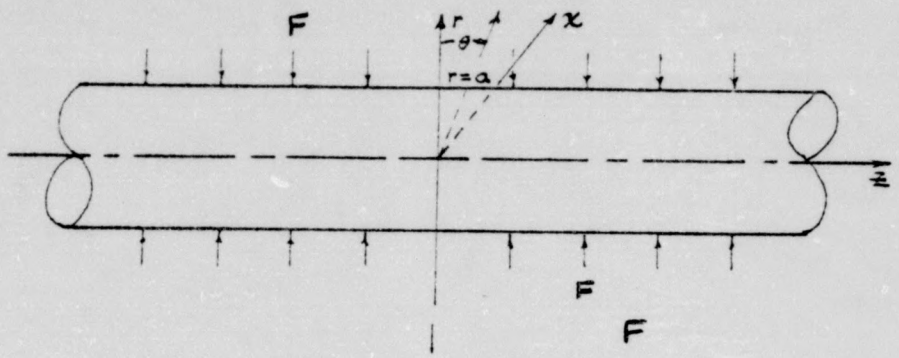


This problem is described by the following equations,

(1) $$\frac{\partial^2 T(r,t)}{\partial r^2} + \frac{1}{r}\frac{\partial T(r,t)}{\partial r} = \frac{1}{\alpha}\frac{\partial T(r,t)}{\partial t}$$ For $0 \le r < a$, $t > 0$

Boundary Conditions $$-k\frac{\partial T(r,t)}{\partial r} = -F$$ $r = a$, $t > 0$

Initial Conditions $$T(r,t) = 0$$ $0 \le r \le a$, $t = 0$

Taking the LaPlace transform of the above equations gives:

$$\int_0^\infty \frac{\partial^2 T(r,t)}{\partial r^2} e^{-st}\,dt + \frac{1}{r}\int_0^\infty \frac{\partial T(r,t)}{\partial r} e^{-st}\,dt = \frac{1}{\alpha}\int_0^\infty \frac{\partial T(r,t)}{\partial t} e^{-st}\,dt$$

(2) $$\frac{d^2 T(r,s)}{dr^2} + \frac{1}{r}\frac{dT(r,s)}{dr} - \frac{s}{\alpha}T(r,s) = 0$$

Boundary Condition $$-k\frac{dT(r,s)}{dr}\bigg|_{r=a} = -\frac{F}{s}$$ $t > 0$

Equation (2) is a modified Bessel equation; therefore, the solution is,

(3) $$T(r,s) = A_n J_o(i\sqrt{\frac{s_n}{\alpha}}\, r)$$

and Boundary Condition

$$-k A_n i\sqrt{\frac{s_n}{\alpha}}\, J_1(i\sqrt{\frac{s_n}{\alpha}}\, a) = -\frac{F}{s}$$

(4) Eliminating $A_n$ and using the inverse LaPlace transform to recover t yields.

$$T(r,t) = -\frac{1}{2\pi i}\int_{\sigma-j\infty}^{\sigma+j\infty} \frac{F\sqrt{\alpha}\; J_o(i\sqrt{\frac{s_n}{\alpha}}\, r)\, e^{st}}{i\, s^{3/2} k\, J_1(i\sqrt{\frac{s_n}{\alpha}}\, a)}\, ds$$

(5) Substituting the series expansions for the Bessel and exponential functions

$$T(r,t) = \frac{1}{2\pi i}\int_{\sigma-j\infty}^{\sigma+j\infty} \frac{F\alpha}{k s^2}\left[\frac{2}{a} - \frac{sa}{4\alpha} + \frac{2s^2a^3}{96\alpha^2} + \frac{2st}{a} - \frac{s^2a^3t}{4\alpha} + \frac{2sr^2}{4a\alpha} - \frac{s^3a^5t^2}{3\alpha} - \cdots\right] ds$$

(6) From the residue theorem

$$T(r,t) = 2\pi i \sum \text{residues}$$

Therefore,

$$T(r,t) = \frac{Fa}{k}\left[\frac{2\alpha t}{a^2} + \frac{r^2}{2a^2} - \frac{1}{4}\right]$$

(7) Now, $J_1\left(i\sqrt{\frac{s}{\alpha}}a\right)$ has simple zeros where $i\sqrt{s/\alpha}\,a = \lambda_n$, where $n = 1, 2, 3, \cdots$ & $\lambda_n$ are positive roots of $J_1\left(i\sqrt{\frac{s}{\alpha}}a\right) = 0$. Thus, the integrand has simple poles at $s = -\lambda_n^2$. Changing the variable from $s$ to $\lambda_n$, (4) can be written

$$T(r,t) = \frac{-1}{2\pi i}\int_{\sigma-j\infty}^{\sigma+j\infty} \frac{2Fa\,J_0(\lambda_n \frac{r}{a})\,e^{-\frac{\alpha\lambda_n^2 t}{a^2}}}{k\lambda_n^2 J_1(\lambda_n)}\,d\lambda_n$$

(8) Using L'Hospital's rule in evaluating the limit and also the fact that $\frac{d}{d\lambda}J_0(\lambda) = -J_1(\lambda)$, then

$$T(r,t) = \frac{-2Fa}{k}\,e^{-\frac{\alpha\lambda_n^2 t}{a^2}}\,\frac{J_0(\lambda_n \frac{r}{a})}{\lambda_n^2 J_0(\lambda_n)}$$

where $\lambda_n$ are the roots of $J_1(\lambda_n) = 0$

(9) Therefore, the complete expression for T(r,t) is

$$T(r,t) = \frac{Fa}{k}\left[\frac{2\alpha t}{a^2} + \frac{r^2}{2a^2} - \frac{1}{4} - \sum_{n=1,2,3,\cdots}^{\infty} 2\,e^{-\frac{\alpha\lambda_n^2 t}{a^2}}\,\frac{J_0(\lambda_n \frac{r}{a})}{\lambda_n^2 J_0(\lambda_n)}\right]$$

## APPENDIX B

Case II - Constant heat flux, F, is applied to the surface of a wire, at time zero, of length L, independent of 0 and the wire connected to a heat sink at Z = 0 and Z = L.

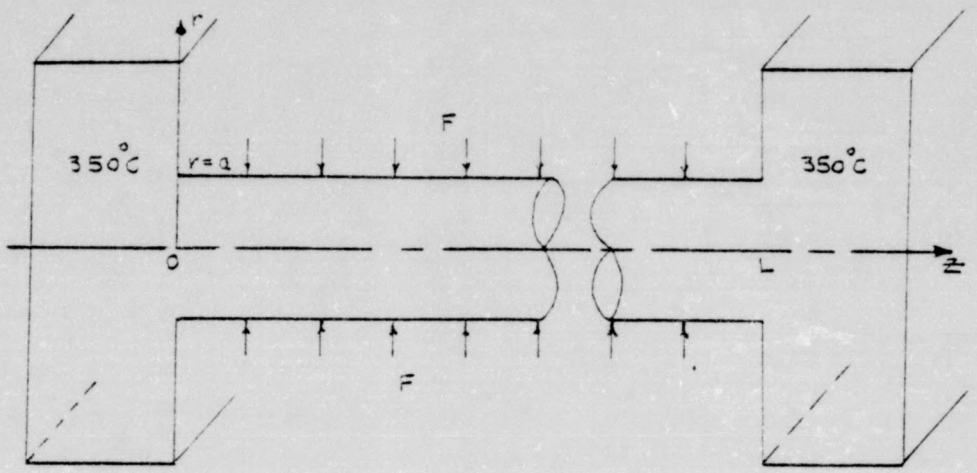


This system is described by the following partial differential equations, boundary and initial condition:

(1) $$\frac{\partial T(z,r,t)}{\partial t} = \alpha \nabla^2 T(z,r,t)$$ For $0 \leq r < a$, $0 < z < L$, $t > 0$

Boundary Condition $T(z,r,t) = 350°C$ $z = 0$ & $z = L$

and $$-F = -k \frac{\partial T(z,r,t)}{\partial r}$$ $r = a$, $0 < z < L$, $t > 0$

Initial Condition $T(z,r,t) = 350°C$ $t = 0$

(2) The LaPlace transform of (1) gives

$$\frac{s}{\alpha} T(z,r,s) - T(z,r,0) = \nabla^2 T(z,r,s)$$

Boundary Condition $$T(L,r,s) = T(0,r,s) = \frac{350}{s}$$

and $$\frac{F}{S} = k \frac{\partial T}{\partial r}(z,a,s)$$

(3) The Fourier transform depresses the Z variable as follows

$$\frac{s}{\alpha}\int_0^L T(z,r,s)\sin\rho z\,dz = \frac{1}{r}\int_0^L \frac{\partial}{\partial r} r\frac{\partial T}{\partial r}(z,r,s)\sin\rho z\,dz + \int_0^L \frac{\partial^2 T}{\partial z^2}(z,r,s)\sin\rho z\,dz$$

let $\rho = \frac{n\pi}{L}$ then $\sin\rho L = \sin n\pi = 0$

and the above equation reduces to

(a) $$\frac{d^2T}{dr^2}(\rho,r,s) + \frac{1}{r}\frac{dT}{dr}(\rho,r,s) - \left(\rho^2 + \frac{s}{\alpha}\right) T(\rho,r,s) = 0$$

Boundary Condition $$\int_0^L \frac{F}{S}\sin\rho z\,dz = k\int_0^L \frac{\partial T}{\partial r}(z,r,s)\sin\rho z\,dz$$

$$-\frac{F}{\rho S}\cos\rho z\Big|_0^L = k\frac{\partial T}{\partial r}(\rho,r,s)$$

(b) $$\therefore\ n = 1,3,5,\cdots \qquad \frac{2F}{\rho S} = k\frac{\partial T}{\partial r}(\rho,r,s)$$

(4) Equation (3) (a) is a modified Bessel equation which has a solution of the form

$$T(\rho, r, s) = A_n J_0\left(i\sqrt{\rho^2 + \frac{s}{\alpha}}\, r\right)$$

This relation substituted in (3) (b) yields the constant An and results in the following equation for T(p,r,s).

$$T(\rho, r, s) = \frac{-2F J_0\left(i\sqrt{\rho^2 + \frac{s}{\alpha}}\, r\right)}{\rho s k i\sqrt{\rho^2 + \frac{s}{\alpha}}\; J_1\left(i\sqrt{\rho^2 + \frac{s}{\alpha}}\, a\right)}$$

(5) The inverse Fourier transform is used to recover the depressed Z variable

$$T(z, r, s) = -\sum_{n=1,3,5\ldots}^{\infty} \frac{4F \sin\frac{n\pi z}{L}\; J_0\left(i\sqrt{\rho^2 + \frac{s}{\alpha}}\, r\right)}{n\pi k \quad s i\sqrt{\rho^2 + \frac{s}{\alpha}}\; J_1\left(i\sqrt{\rho^2 + \frac{s}{\alpha}}\, a\right)}$$

(6) The inverse LaPlace transform yields the temperature T as a function of time

$$T(z, r, t) = \sum_{n=1,3,5\ldots}^{\infty} \frac{4F \sin\frac{n\pi z}{L}}{n\pi k}\; \frac{1}{2\pi i} \int_{\sigma-j\infty}^{\sigma+j\infty} \frac{-J_0\left(i\sqrt{\rho^2 + \frac{s}{\alpha}}\, r\right) e^{st}}{s i\sqrt{\rho^2 + \frac{s}{\alpha}}\; J_1\left(i\sqrt{\rho^2 + \frac{s}{\alpha}}\, a\right)}\, ds$$

let $$\beta = \frac{-1}{2\pi i} \int_{\sigma-j\infty}^{\sigma+j\infty} \frac{J_0\left(i\sqrt{\rho^2 + \frac{s}{\alpha}}\, r\right) e^{st}\, ds}{s i\sqrt{\rho^2 + \frac{s}{\alpha}}\; J_1\left(i\sqrt{\rho^2 + \frac{s}{\alpha}}\, a\right)}$$

(7) The residues of integrand of $\beta$ at poles $s = 0 \quad \xi_i' - \alpha p^2$ are as follows

$$\lim_{s \to 0} \left\{ \frac{-J_0(i\sqrt{p^2}r)\, e^{st}}{i\sqrt{p^2}\, J_1(i\sqrt{p^2}a)} \right\} = \frac{-J_0(ipr)}{ipJ_1(ipa)} = \frac{I_0(pr)}{pI_1(pa)}$$

$$\lim_{s \to -\alpha p^2} \frac{\frac{\partial}{\partial s}\left(s + \alpha p^2\right)}{\frac{\partial \lambda}{\partial s}\frac{\partial}{\partial \lambda} i\sqrt{p^2 + \frac{s}{\alpha}}\, J_1\left(i\sqrt{p^2 + \frac{s}{\alpha}}a\right)} \quad \frac{e^{-\alpha p^2 t}}{\alpha p^2} =$$

$$\lim_{s \to -\alpha p^2} \left\{ \frac{e^{-\alpha p^2 t}}{\alpha p^2 a\, i\sqrt{p^2 + \frac{s}{\alpha}}\; J_0\left(i\sqrt{p^2 + \frac{s}{\alpha}}a\right) \frac{i}{2} \frac{\sqrt{}}{\alpha\sqrt{p^2 + \frac{s}{\alpha}}}} \right\} = \frac{-2e^{-\alpha p^2 t}}{a p^2}$$

$$\lim_{s \to -\alpha\left[\frac{\lambda_n^2}{a^2} + p^2\right]} \left\{ \frac{s + \alpha\left[\frac{\lambda_n^2}{a^2} + p^2\right]}{i\sqrt{p^2 + \frac{s}{\alpha}}\, J_1\left(i\sqrt{p^2 + \frac{s}{\alpha}}a\right)} \right\} \left\{ \frac{-J_0\left(i\sqrt{p^2 + \frac{s}{\alpha}}r\right) e^{st}}{s} \right\} =$$

$$\frac{-2\, J_0\left(\lambda_n \frac{r}{a}\right) e^{-\alpha\left[\frac{\lambda_n^2}{a^2} + p^2\right]t}}{a\, J_0(\lambda_n)\left(\frac{\lambda_n^2}{a^2} + p^2\right)}$$

(8) Therefore, since $T(Z,r,t)$ is equal to $2\pi i$ times the sum of the residues

$$T(z,r,t) = \sum_{n=1,3,\cdots}^{\infty} \frac{4F\sin(\rho z)}{n\pi k}\left\{\frac{I_0(\rho r)}{\rho I_1(\rho a)} - \frac{2e^{-\alpha\rho^2 t}}{a\rho^2} - \frac{2J_0(\lambda_m \frac{r}{a})e^{-\alpha\left[\frac{\lambda_m^2}{a^2}+\rho^2\right]t}}{a J_0(\lambda_m)\left(\frac{\lambda_m^2}{a^2}+\rho^2\right)}\right\}$$

where $\rho = \frac{n\pi}{L}$ and $\lambda_m$ are the positive roots of $J_1(\lambda_m) = 0$

## APPENDIX C

Case III - Pulses of heat flux, F(t), are applied to the surface of a wire starting at time zero. The flux is independent of $\theta$ and the wire is connected to a heat sink at Z = 0 and Z = L. Case III is the same as Case II except the excitations are pulses as follows:

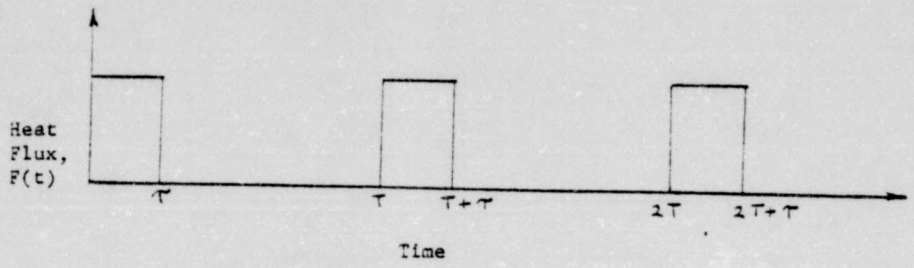


This case is described by the following set of equations:

(1) $$\frac{\partial T(z,r,t)}{\partial t} = \alpha \nabla^2 T(z,r,t) \qquad \begin{matrix} 0 \le r < a \\ 0 < z < L \\ t > 0 \end{matrix}$$

(b) Boundary Condition $T(z,r,t) = 350^\circ C \qquad z = 0 \text{ & } z = L$

(b) and $$F(t) = -k \frac{\partial T(z,r,t)}{\partial r} \qquad \begin{matrix} r = a \\ 0 < z < L \\ t > 0 \end{matrix}$$

Where F(t) is on $\tau$ seconds and off $T - \tau$, repeating every $nT$ seconds

(c) Initial Condition $T(z,r,t) = 350^\circ C \qquad t > 0$

(2) Because the boundary heat flux is in the form of pulses, the form of the boundary equation is changed to a Dirac or impulse function. The temperature function is derived and the convolution integral used to generate the rectangular shape.

The boundary equation written in terms of the Dirac function is:

$$\delta(t) = -k \frac{\partial T(z,r,t)}{\partial r} \qquad \begin{matrix} r=a \\ 0<z<1 \\ t>0 \end{matrix}$$

(3) Taking the LaPlace transform of (1) and (2) gives

$$sT(z,r,s) - T(z,r,0) = \alpha \nabla^2 T(z,r,s) \qquad \begin{matrix} 0 \le r < a \\ 0 < z < L \end{matrix}$$

Boundary Condition $$1 = k \frac{\partial T}{\partial r}(z,r,s) \qquad \begin{matrix} r=a \\ 0<z<L \end{matrix}$$

The temperature of the frame and the initial condition is chosen to be zero and the 350°C is added to the solution after the temperature relation is derived.

(4) The Fourier Sine transform suppresses the Z variable which yields the following ordinary differential equations

$$\frac{d^2 T(\rho, r, s)}{dr^2} + \frac{1}{r}\frac{dT(\rho, r, s)}{dr} - \left(\rho^2 + \frac{s}{\alpha}\right) T(\rho, r, s) = 0$$

With the boundary condition

$$\frac{2}{\rho} = k \left.\frac{\partial T(\rho, r, s)}{\partial r}\right|_{r=a}$$

(5) This equation is a modified Bessel equation and the technique used in Case II generates a solution

$$T(z, r, t) = \frac{-4}{\pi k}\frac{1}{2\pi i}\int_{\sigma - j\infty}^{\sigma + j\infty} \sum_{n=1,3,\ldots} \frac{J_0\left(i\sqrt{\rho^2 + \frac{s}{\alpha}}\, r\right) \sin\frac{n\pi z}{L}\, e^{st}\, ds}{i\sqrt{\rho^2 + \frac{s}{\alpha}}\; J_1\left(i\sqrt{\rho^2 + \frac{s}{\alpha}}\, a\right) n}$$

(6) Using the Residue Theorem and complex variable theory (see pp. 46 and 47), the temperature of the grid laterial wire is

$$T(z, r, t) = \sum_{n=1,3,\ldots}^{\infty} \frac{3\alpha \sin\frac{n\pi z}{L}}{n\pi k a}\left\{ e^{-\alpha \rho^2 t} + \sum_{m=1,2,} \frac{J_0\left(\lambda_m \frac{r}{a}\right)}{J_0(\lambda_m)}\, e^{-\alpha\left(\frac{\lambda_m^2}{a^2} + \rho_n^2\right) t} \right\}$$

Where $\rho = \frac{n\pi}{L}$ and $\lambda_m$ are the positive roots of $J_1(\lambda_m) = 0$

(7) Checking equation (6) for correctness.

(a) The dimensions of $\alpha$, $Z$, $L$, $k$, $a$, $r$, $\xi$, $t$ were substituted in (6) and T(Z,r,t) reduces to $[^{\circ}c]$

(b) Equation (6) substituted in

$$\frac{\partial T}{\partial t}(z,r,t) = \alpha \nabla^2 T(z,r,t)$$

from (1), reduces this original equation to an identity.

(c) Substituting (6) in

$$\delta(t) = -k \frac{\partial T}{\partial r}(z,r,t)\Bigg|_{r=a}$$

reveals the boundary condition is satisfied or substituting Z = 0 and L satisfies the temperature at the frame.

(d) Also, reasoning physically, $\frac{\partial T}{\partial r}(z,r,t)$, should be zero at $r = 0$ because of symmetry; i.e., heat flow through the center of the wire is zero. Taking $\frac{\partial}{\partial r}(6)$ and substituting $r = 0$ reveals $q/A$ is zero.

(e) Substituting $t = 0$ in equation (6) reduces this equation to zero or any chosen constant since these equations are linear differential equations.

(8) Therefore, equation (6) is a solution to equation (1) and satisfies the assumed boundary conditions. Equation (6) can be written as

$$h(z,r,t) = K_n\left[e^{-\beta t} + K_m e^{-\gamma t}\right]$$

Where

$$K_n = \sum_{n=1,3,..}^{\infty} \frac{8\alpha \sin(\rho_n z)}{\pi n k a}$$

$$K_m = \sum_{m=1,2,3,..}^{\infty} \frac{J_o(\lambda_m \frac{r}{a})}{J_o(\lambda_m)}$$

$$\beta = \alpha \rho_n^2$$

$$\gamma = \alpha\left(\frac{\lambda_m^2}{a^2} + \rho_n^2\right)$$

$$\rho_n = \frac{n\pi}{L}$$

and $J_1(\lambda_m) = 0$ give the positive roots $\lambda_m$

Notice that the temperature response has been changed to $h(z,r,t)$ for an impulse excitation, which is standard notation. At a certain position and radius, Z and r would be fixed and the expression $h(z,r,t) = h(t)$.

(9) The convolution integral is an important analytical tool in transform theory and is defined as

$$\int_0^t f(t-\lambda)\, g(\lambda)\, d\lambda$$

Using the convolution integral combined with the Dirac function, a function e(t) can be thought of as the sum of an infinite number of Dirac or $\delta$-functions. The area under each being the value of e(t) at the time the $\delta$-function is considered; i.e.,

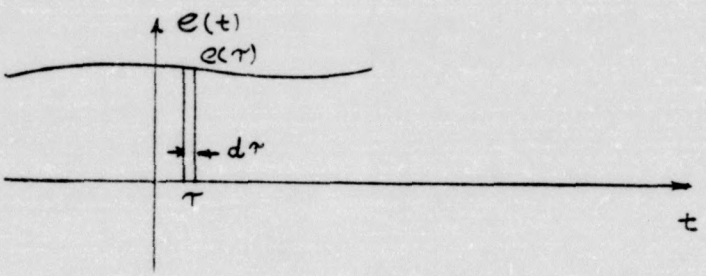


$$e(t) = \int_0^t e(\tau)\, \delta(t-\tau)\, d\tau$$

(10) Equation (8) is an equation that is the impulse response of a wire, heat sinked at each end, to an impulse of excitation. This impulse response can be converted to any excitation by using the convolution integral. For a rectangular excitation the relation is

$$T(z,r,t) = \int_0^t F(\tau)\, h(t-\tau)\, d\tau$$

(11) When a rectangular pulse of heat flux, F, is applied to the surface of the wire, the temperature is calculated, knowing the impulse response as follows,

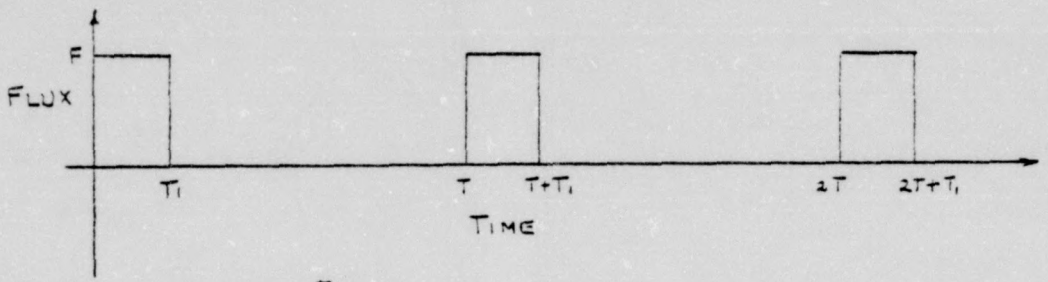


$$T(z,r,t) = \int_0^t F(\tau)\, h(t-\tau)\, d\tau$$

$$= \int_0^t F\left\{ 1(t) - 1(t-T_1) \cdots \right\} K_n \left[ e^{-\beta(t-\tau)} + K_m e^{-\gamma(t-\tau)} \right] d\tau$$

$$= F K_n \left\{ \frac{1}{\beta}\left[1 - e^{-\beta t}\right] + \frac{K_m}{\gamma}\left[1 - e^{-\gamma t}\right] - \frac{1}{\beta}\left[1 - e^{-\beta(t-T_1)}\right] - \frac{K_m}{\gamma}\left[1 - e^{-\gamma(t-T_1)}\right] \right\}$$

$K_n$, $K_m$, $\beta$, $\gamma$, $p_n$ are defined on p. 53 and this equation is shown as a solution to Case III on page 20.

## APPENDIX D

The computer program for Case III, equation (12), page 20, is as follows in basic language. Some changes were required in the symbols shown on page 15.

r = R = VARIABLE DISTANCE FRØM THE CENTER ØF THE GRID WIRE

a = D = RADIUS ØF THE LATERAL WIRE

z = Z = VARIABLE DISTANCE FRØM THE GRID FRAME

L = C = LENGTH ØF THE LATERAL WIRE

t = T = TIME

X7 = TEMPERATURE ØF THE GRID LATERAL WIRE AS A FUNCTIØN ØF Z, R, T = T(z,r,t)

To = 350° C = STEADY STATE TEMPERATURE

F = Q/A = CØNSTANT HEAT FLUX

k = K = HEAT CØNDUCTIVITY ØF THE GRID WIRE

α = A = THERMAL DIFFUSIVITY ØF THE GRID WIRE

A = 2πRC = SURFACE AREA ØF THE GRID WIRE

$\lambda_n$ = M(M) = PØSITIVE RØØTS ØF $J_1(\lambda_n) = 0$

Jo = J(M(M)) = BESSEL FUNCTIØN, ØRDER 0

π = E = PI = 3.14159

T1 = PERIØD ØF PULSES

τ = V8 = TIME PULSE IS ØN

Q = PØWER EXCITATIØN TØ THE GRID

N1 = NUMBER ØF PULSES

N = SUMMATIØN DUMMY VARIABLE

```
50 LET N2=50
100 DIM P(25)
110 DIM B(25)
120 DIM I(20),G(20)
130 DIM X(25)
140 READ A,K,C,D,E
150 DATA .471,.3,.762,.000762,3.14159
160 READ T1, V8
165 DATA .2,.1
170 LET Q=.05
180 LET K=K*4.185
190 LET F=30
200 FOR M= 1 TO 9
210 READ M(M)
220 NEXT M
230 DATA 3.832, 7.016, 10.173, 13.324
235 DATA 16.472, 19.616, 22.76, 25.904
240 LET S=8*Q*A/(K*2*E^2*D^2*C)
250 FOR Z=.381 TO .762 STEP .1905
260 PRINT "            R            Z  "
270 PRINT USING 280, Z
280:                                  #.#######
290 FOR R=0 TO .00001
300 PRINT USING 310,R
310:          #.######
320 PRINT  " TIME ", " PULSE NO. ", " TEMP "
330 FOR M= 1 TO 7
340 LET J=0
350 FOR H=0 TO F
360 LET L(M)=M(M)*R/B
370 LET P=(L(M)/2)^(2*H)
380 LET D1=1
390 FOR Y= 1 TO H
400 IF H=0 THEN 430
410 LET D1=D1*Y
420 NEXT Y
430 LET D2=D1^2
440 LET A1=P/D2
450 LET B=(-1)^H*A1
460 LET J(M)=J+B
470 LET J=J(M)
480 IF H=0 THEN 540
490 LET V=ABS(J)
500 LET W=U-V
510 LET W=ABS(W)
520 IF W<.0001 THEN 550
530 LET U= ABS(J)
540 NEXT H
550 NEXT M
560 LET M=0
570 LET U=0
```

```
580 LET B=0
590 FOR M= 1 TO 7
600 LET D=0
610 FOR H=0 TO F
620 LET P=(M(M)/2)^(2*H)
630 LET D1=1
640 FOR Y= 1 TO H
650 IF H=0 THEN 680
660 LET D1=D1*Y
670 NEXT Y
680 LET D2=D1^2
690 LET A1=P/D2
700 LET B=(-1)^H*A1
710 LET O(M)=O+B
720 LET D=O(M)
730 IF H=0 THEN 790
740 LET V=ABS(O)
750 LET W=U-V
760 LET W=ABS(W)
770 IF W<.0001 THEN 800
780 LET U= ABS(O)
790 NEXT H
800 NEXT M
810 LET Y4=0
820 FOR N1=0 TO 20
830 LET A2=(-1)^N1
840 LET B3=INT((N1+.001)/2)
850 LET E1=(-1)^(N1+1)
860 LET D4=.05
870 LET B1=INT((N1+1+.001)/2)*T1+V8/2+(-1)^(N1+2)*V8/2
880 LET B2=D3*T1+V8/2+E1*V8/2
890 FOR T=B2 TO B1 STEP D4
900 IF T<1-.0001 THEN 920
910 IF T>B1 -.00001 THEN 1200
920 LET X7=0
930 FOR N= 1 TO 5 STEP 2
940 LET P(N)=N*E/C
950 LET B(N)=S*SIN(N*E*Z/C)/N
960 FOR M1=0 TO N1 STEP 1
970 LET X4=0
980 LET X6=0
990 LET G=INT((M1+.001)/2)*T1+V8/2+(-1)^(M1+1)*V8/2
1000 FOR M= 1 TO 3
1010 LET X8=A*(M(M)^2/D^2+P(N)^2)
1015 LET G1=T-G
1020 LET X9=X8*(T-G)
1030 IF X9>30 THEN 1060
1035 LET Y1=B(N)*J(M)*(-1)^M1/(O(M)*X8)
1040 LET X4=X4+B(N)*J(M)*(-1)^M1/(O(M)*X8)*(1-EXP(-X9
1070 NEXT M
1080 LET X3=A*P(N)^2
1090 LET X5=X3*(T-G)
1100 IF X5>30 THEN 1130
1110 LET X6=X6+B(N)*(-1)^M1/X3*(1-EXP(-X5))
```

```
1115 LET Y2=B(N)*(-1)^M1/X3
1120 GO TO 1140
1130 LET X6=X6+(-1)^M1*B(N)/X3
1135 LET Y2=B(N)*(-1)^M1/X3
1140 LET X7=X7+X4+X6
1150 NEXT M1
1160 NEXT N
1170 LET X7=X7+350
1180 PRINT USING 1185,I,N1,X7
1185:  #####.#####    ##.##   #####.#####
1190 NEXT I
1200 NEXT N1
1210 NEXT R
1220 NEXT Z
1230 END
RUN
```

Z
.3810000

R
.000

| TIME | PULSE NO. | TEMP |
|---|---|---|
| .0 | .00 | 350.000000 |
| .05 | .00 | 680.746880 |
| .1 | .00 | 921.893710 |
| .1 | 1.00 | 921.893710 |
| .15 | 1.00 | 753.436060 |
| .2 | 1.00 | 621.061740 |
| .2 | 2.00 | 621.061740 |
| .25 | 2.00 | 862.410800 |
| .3 | 2.00 | 1043.631300 |
| .3 | 3.00 | 1043.631300 |
| .35 | 3.00 | 835.015180 |
| .4 | 3.00 | 675.729740 |
| .4 | 4.00 | 675.729740 |
| .45 | 4.00 | 899.045040 |
| .5 | 4.00 | 1068.180700 |
| .5 | 5.00 | 1068.180700 |
| .55 | 5.00 | 851.466310 |
| .6 | 5.00 | 686.744010 |
| .6 | 6.00 | 686.744010 |
| .65 | 6.00 | 906.432650 |
| .7 | 6.00 | 1073.131300 |
| .7 | 7.00 | 1073.131300 |
| .75 | 7.00 | 854.783810 |
| .8 | 7.00 | 688.977140 |
| .8 | 8.00 | 688.977140 |
| .85 | 8.00 | 907.922420 |
| .9 | 8.00 | 1074.129700 |
| .9 | 9.00 | 1074.129700 |
| .95 | 9.00 | 855.452810 |
| 1.0 | 10.00 | 689.425460 |
| 1.05 | 10.00 | 908.222250 |

## APPENDIX E

Forty tubes, GE18651 planar power triodes, were given an increasing grid excitation until a change in cutoff potential suggested open or distorted grid wires. The tubes were broken and the grids removed for examination. The turns are numbered from 1 through 62 (see sketch below). The damaged turns were recorded, and an estimate was made relative to what caused the grid wire damage, Table II. A photograph of two grids excited with 8 and 8.1 watts is shown on page 62.

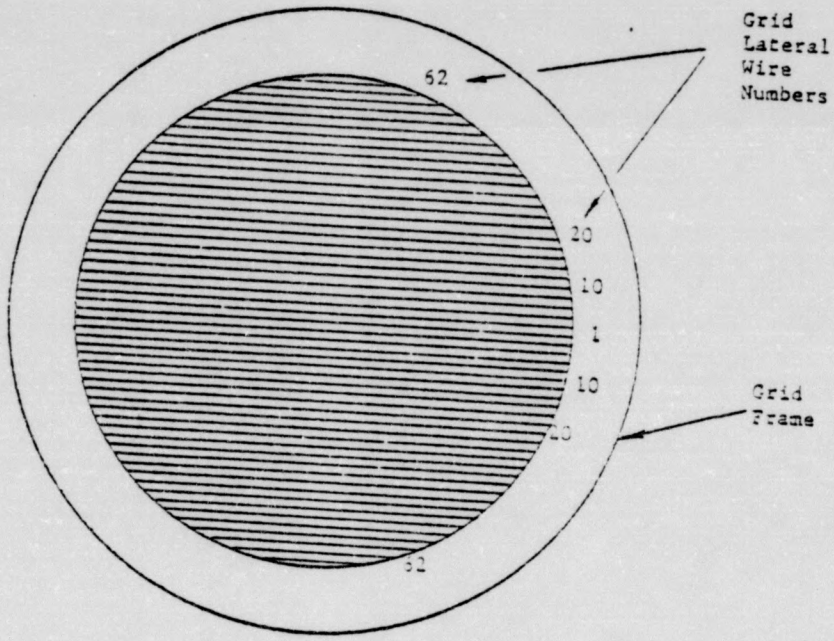


### Test Conditions

| | | | | | |
|---|---|---|---|---|---|
| Preheat: | Ef = 6.3 V<br>If = 500 mA | Ep = 200 V<br>Ip = 20 mA | | IpCO: | Ep = 200 V<br>Eg = -7 V |

| Lot | Tube No. | Grid Power Watts | Numbered Turns Burnt Open | Remarks |
|---|---|---|---|---|
| F30 | 175 | 4.0 | 30-45 | 10 turns shorted to cathode |
| F30 | 95 | 4.0 | 20-40 | 15 turns shorted to cathode |
| F30 | 197 | 4.8 | Grid Destroyed | |
| F30 | 191 | 5.0 | 42-45 | 3 turns shorted to cathode |
| F30 | 245 | 5.0 | 45-60 | 6 turns open |
| F30 | 251 | 5.0 | 40-50 | 4 turns shorted to cathode |
| F30 | 246 | 6.0 | 6 | Open |
| F30 | 167 | 6.0 | 40-42 | 2 turns open |
| F30 | 215 | 6.2 | 50-60 | 3 turns open |
| F30 | 245 | 6.2 | None | |
| F30 | 173 | 6.4 | None | |
| F30 | 150 | 6.5 | 45-50 | 4 turns shorted to cathode |
| F30 | 96 | 6.6 | 44-50 | 3 turns shorted to cathode |
| F30 | 100 | 7.0 | None | |
| F30 | 155 | 7.0 | 40-50 | 5 turns shorted to cathode |
| F30 | 103 | 7.0 | 1-10 | Evidence of hot turns |
| F30 | 218 | 7.0 | 30-32 & 54-56 | Open, shorted? |
| F30 | 224 | 7.0 | 7-9 | Open |
| F33 | 45 | 7.0 | 30,34,36 | Open |
| F33 | 235 | 7.2 | 9,11,12,13 | Open |
| F33 | 139 | 7.2 | | Grid discolored in center |
| F32 | 229 | 8.0 | 4,5 | Open |
| F33 | 10 | 8.0 | 34 | Open |
| F33 | 249 | 8.0 | 1-5 | Open, 1 or 2 shorted |
| F32 | 160 | 8.0 | 1,2,13,14,15 | Open |
| F30 | 190 | 8.1 | 30-46 | 7 turns shorted to cathode |
| F30 | 166 | 8.1 | 1,2,3 | Slack due to high temperature |
| F30 | 210 | 8.1 | 1,2,3,4 | Open |
| F32 | 250 | 8.1 | 1-5 | Evidence of hot turns |
| F33 | 15 | 8.1 | 44-47 | Shorted to cathode |
| F32 | 153 | 8.1 | 30-35 | Shorted to cathode |
| F33 | 110 | 8.1 | 12-17 | Open |
| F31 | 244 | 8.1 | 11-15 | Open |
| F32 | 268 | 8.1 | 32,33 | Open |
| F32 | 159 | 8.2 | 30-33 | Open |
| F33 | 63 | 8.4 | 6,7,8,12 | Open |
| F30 | 222 | 8.45 | 33 | Open |
| F32 | 283 | 8.5 | 30-35 | Open |
| F30 | 195 | 8.7 | 1,2 | Slack |
| F30 | 162 | 9.5 | 1-12 | 8 open turns |

Table II — An Examination of Grids Taken From Tubes Subjected to High Grid Dissipations

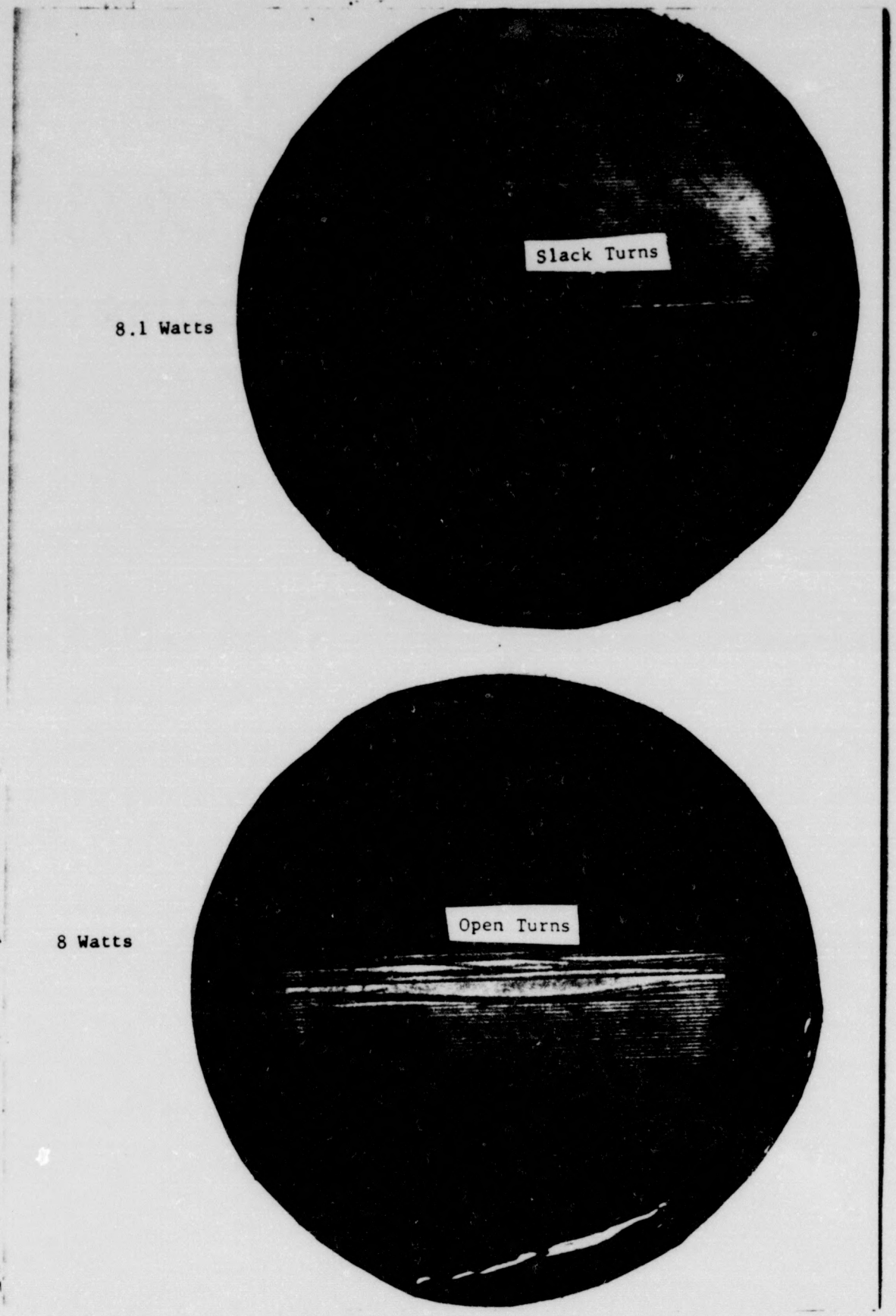


II - Grids Taken from Microwave Triode Showing Damaged Lateral Wires

# LIST OF REFERENCES

1. Rush, J.W., "Performance and Application of Microwave Gridded Vacuum Tubes and Microwave Circuit Modules," Tube Products Department, Owensboro, Kentucky, May (1965).

2. Terman, F.E., Radio Engineering, Third Edition, Chap. 7, p. 394, (McGraw-Hill Book Co., New York, 1947).

3. McAdams, W.H., Heat Transmission, Third Edition, Chap. 3, p. 49, (McGraw-Hill Book Co., New York, 1933).

4. Hildebrand, F.B., Advanced Calculus for Applications, First Edition, Chap. 9, p. 429 (Prentice-Hall, Inc., Englewood Cliffs, New Jersey, 1962)

5. Hildebrand, F.B., Methods of Applied Mathematics, Second Edition, Chap. 3, p. 237 (Prentice-Hall, Inc., Englewood Cliffs, New Jersey, 1965)

6. Wylie, C.R., Advanced Engineering Mathematics, Second Edition, Chap. 8, p. 334 (McGraw-Hill Book Co., New York, 1960)

7. Tranter, C.J., Integral Transforms in Mathematical Physics, Third Edition, Chap. 6, p. 83 (John Wiley and Sons, New York, 1955)